UNIVERSITI MALAYSIA PAHANG

BORANG PENGESAHAN STATUS TESIS◆

JUDUL: **PREDICTION OF GRINDING MACHINABILITY WHEN GRIND P20 TOOL STEEL USING WATER BASED ZnO NANO-COOLANT**

SESI PENGAJIAN: 2011/2012

Saya, **YOGESWARAN A/L MUTHUSAMY (881209-01-5311)**

mengaku membenarkan tesis (Sarjana Muda / ~~Sarjana / Doktor Falsafah~~)* ini disimpan di perpustakaan dengan syarat-syarat kegunaan seperti berikut:

1. Tesis ini adalah hakmilik Universiti Malaysia Pahang (UMP).
2. Perpustakaan dibenarkan membuat salinan untuk tujuan pengajian sahaja.
3. Perpustakaan dibenarkan membuat salinan tesis ini sebagai bahan pertukaran antara institusi pengajian tinggi.
4. **Sila tandakan (√)

	SULIT	(Mengandungi maklumat yang berdarjah keselamatan atau kepentingan Malaysia seperti yang termaktub di dalam AKTA RAHSIA RASMI 1972)
	TERHAD	(Mengandungi maklumat TERHAD yang telah ditentukan oleh organisasi / badan di mana penyelidikan dijalankan)
√	**TIDAK TERHAD**	

Disahkan oleh:

_____
(TANDATANGAN PENULIS)

_____
(TANDATANGAN PENYELIA)

Alamat Tetap:
No 246 Jalan Pinang 1,
Taman Kota Kulai,
81000 Kulai,
Johor

Engr. Dr. Kumaran Kadirgama

(Nama Penyelia)

Tarikh: **15 JUNE 2012**

Tarikh: **15 JUNE 2012**

CATATAN: * Potong yang tidak berkenaan.

** Jika tesis ini SULIT atau TERHAD, sila lampirkan surat daripada pihak berkuasa/organisasi berkenaan dengan menyatakan sekali tempoh tesis ini perlu dikelaskan sebagai SULIT atau TERHAD.

◆ Tesis dimaksudkan sebagai tesis bagi Ijazah Doktor Falsafah dan Sarjana secara Penyelidikan, atau disertasi bagi pengajian secara kerja kursus dan penyelidikan, atau Laporan Projek Sarjana Muda (PSM).

PREDICTION OF GRINDING MACHINABILITY WHEN GRIND P20
TOOL STEEL USING WATER BASED ZnO NANO-COOLANT

YOGESWARAN S/O MUTHUSAMY

Report submitted in partial fulfillment of the requirement
for the award of Bachelor of Mechanical Engineering

Faculty of Mechanical Engineering
UNIVERSITI MALAYSIA PAHANG

JUNE 2012

UNIVERSITI MALAYSIA PAHANG
FACULTY OF MECHANICAL ENGINEERING

I certify that the project entitle "Prediction of Grinding Machinability when Grind P20 Tool Steel using Water Based ZnO Nano-Coolant" is written by Yogeswaran S/O Muthusamy. I have examined the final copy of this project and in my opinion; it is fully adequate in terms of scope and quality for the award of the degree of Bachelor of Engineering. I herewith recommend that it be accepted in partial fulfillment of the requirement for the degree of Bachelor of Mechanical Engineering.

MR. NASRUL HADI JOHARI

         Examiner   Signature

SUPERVISOR'S DECLARATION

I hereby declare that I have checked this project and in my opinion, this project is adequate in terms of scope and quality of this thesis is qualified for the award of the Bachelor of Mechanical Engineering.

Signature   :

Name   : Engr. Dr. KUMARAN KADIRGAMA

Position   : HEAD OF DEPARTMENT (BIOMECHANICAL)

Date   : 15 JUNE 2012

STUDENT'S DECLARATION

I hereby declare that the work in this thesis is my own except for quotations and summaries which have been duly acknowledged. The thesis has not been accepted for any degree and is not concurrently submitted for award of other degree.

Signature   :

Name   : YOGESWARAN S/O MUTHUSAMY

ID Number   : ME08076

Date   : 11 JUNE 2012

DEDICATION

I specially dedicate to my beloved parents

and those who have guided and

motivated me for this project

ACKNOWLEDGEMENT

First and foremost, the deepest sense of gratitude to the God, who guide and gave me the strength and ability to complete this final year project successfully. Infinite thanks I brace upon Him. I would like to express my sincere gratitude to my supervisor Dr. Kumaran Kadirgama for his continuous guidance, support and encouragement, which gave me huge inspiration in accomplishing this research. His practice of professional ethics and conducts which encourages me to become confident and competent person to work individually as well as in group.

Besides that, I also took this opportunity to thank Mr.Aziha who helped me a lot in my experiment. He also very supportive in exploring the features and utilization of grinding machine besides allows to use the laboratory until late hour. A sincere appreciation to Mr. Zulfahmi, UMP Central Lab instructor who help me a lot in using Scanning Electron Microscope.

. Other than that, Mr. Nasrul Hadi Johari, who reviewed and certified that my thesis is fully adequate in terms of scope and quality for the award of the degree of Bachelor of Engineering. Not forgot to thank the panels who critics the outcome of this research besides providing some suggestions to improve the discussion and conclusion as well. I would also like to express my deepest appreciation to my parents whom always support and motivate me to complete this research and thesis. I also owe a depth of gratitude to my university friends who shared their knowledge and ideas that lead to the completion of this thesis.

Finally, to individuals who has involved neither directly nor indirectly in succession of this research with thesis writing. Indeed I could never adequately express my indebtedness to all of them. Hope all of them stay continue support me and give confidence in my efforts in future. Thank you

ABSTRACT

Grinding is often an important finishing process for many engineering components and for some components is even a major production process. The surface roughness, R_a is also an important factor affecting many manufacturing departments. In this study, a model have been developed to find the effect of grinding condition which is depth of cut, type of wheel and type of grinding coolant on the surface roughness on AISI P20 tool steel and wheel wear. Besides that, the objective of this study is to determine the effect of Zinc Oxide (ZnO) nano-coolant on the grinding surface quality and wheel wear for various axial depth. Precision surface grinding machine is used to grind the AISI P20 tool steel. The work table speed would be constant throughout the experiment which is 200 rpm. The experiment conducted with grinding depth in the range of 5 to 21µm. Besides, Aluminum Oxide wheel and Silicon Carbide wheel are used to grind the work piece in this experimental study. Next, the experiment will conduct using ZnO nano-coolant. Finally, the artificial intelligence model has been developed using ANN. From the result, it shows that the lower surface roughness and wheel wear obtain at the lowest cutting depth which is 5 µm. Besides that, grind using ZnO nano-coolant gives better surface roughness and minimum wheel wears compare to grind using water based coolant. From the prediction of ANN, it shows that the surface roughness became constant after cutting depth 21 µm. In conclusion, grind using ZnO nano-coolant with cutting depth 5 µm obtain a better surface roughness and lowest wheel wear. As a recommendation, various machining can be conducted using ZnO nano-coolant to emphasize better results.

ABSTRAK

Pengisaran adalah sering suatu proses yang penting untuk banyak komponen kejuruteraan dan untuk beberapa komponen lain. Kekasaran permukaan, adalah juga merupakan faktor penting yang mempengaruhi banyak jabatan pembuatan. Dalam kajian ini, satu model telah dihasilkan untuk mencari kesan keadaan pengisaran iaitu ketebalan potongan, jenis roda pengisar dan jenis bahan penyejuk yang memberi kesan kepada kekasaran permukaan keluli AISI P20 dan juga kehausan roda mesin pengisar. Selain itu, objektif utama kajian ini adalah untuk menentukan kesan nano-penyejuk ZnO pada kualiti permukaan pengisaran dan kehausan roda pengisar. Mesin pengisaran permukaan persis digunakan untuk mengisar alat kerja keluli AISI P20. Kelajuan mesin akan menjadi malar sepanjang eksperimen dijalankan iaitu 200 rpm. Eksperimen dijalankan dengan kedalaman pengisaran dalam lingkungan 5 hingga 21μm. Selain itu, roda Aluminium Oksida dan Silikon Karbida roda digunakan untuk mengisar bahan kerja dalam kajian ini. Seterusnya, eksperimen akan dijalankan menggunakan nano-penyejuk ZnO. Akhir sekali, satu model telah dibangunkan dengan menggunakan ANN. Kajian ini menunjukan bahawa kekasaran permukaan yang paling rendah diperolehi pada kedalaman pepotogan yang rendah iaitu 5 μm. Selain itu, eksperimen yang dijalankan menguna nano-penjejuk ZnO memperolehi kekasaran permukaan yang lebih baik dan kahausan roda yang minimum berbanding dengan mengisar mengunakan penjejuk berasaskan air. Dari ramalan ANN, ia menunjukkan bahawa kekasaran permukaan menjadi malar selepas pemotongan 21 μm. Kesimpulannya, kisar menggunakan nano-penyejuk ZnO dengan kedalaman pemotongan 5 μm mendapatkan kekasaran permukaan yang lebih baik dan kehausan roda paling rendah. Sebagai saranan, pelbagai mesin boleh dijalankan dengan menggunakan nano-penyejuk ZnO untuk memperolehi keputusan yang lebih baik.

TABLE OF CONTENTS

LIST OF TABLES

LIST OF FIGURES

LIST OF SYMBOL

μm	Micro Meter
%	Percentage
°C	Degree Celcius
$\varnothing$	Volume percentage of nano particle
$\varnothing_2$	Volume percentage of nano-coolant after dilute
φ	Weight percentage of nano particle
ρ_w	Density of Water
ρ_p	Density of Nano particle
ΔV	Total amount of distill water to be added
C_v	Specific Heat
Cm	Centimeter
g/cm^3	Gram per centimeter cubic
k	Thermal Conductivity
kg	Kilogram
kg/mm	Kilogram per milimeter
kg/m^3	Kilogram per meter cubic
K	Kelvin
l	Litre
mm	Milimeter
mm^3	Milimeter cubic
m/min	Meter per minutes
m/s	meter per second
rpm	Revolution per minute
W/m-K	Watt per meter Kelvin

LIST OF ABBREVIATION

ADC	Analog to Digital Converter
AE	Absolute Error
Al_2O_3	Aluminum Oxide
ANN	Artificial Neural Network
ARE	Absolute Relative Error
EG	Ethylene Glycol
EHT	Electron High Tension
EVO	Evolution
FKM	Fakulti Kejuruteraan Mekanical
GMDH	Group Method of Data Handling
HN	Hardness Number
Mag	Magnification
MSE	Mean Square Error
RSM	Response Surface Method
SiC	Silicon Carbide
WB	Water Based
WD	Working Distance
ZnO	Zinc Oxide
ZrO_2	Zirconium Oxide

LIST OF APPENDICES

CHAPTER 1

INTRODUCTION

1.1   Project Brackground

The grinding machinability is widely used in the manufacturing of various materials (Samek et al., 1996). Grinding is often an important finishing process for many engineering components and for some components is even a major production process. There are many different types of grinding parameters. Different types of parameter in grinding process will be the effect of the characteristic of the work piece such as surface roughness, temperature, wheel wear, force and others. There are many types of parameters in the grinding process. Some of the parameters may be measured while the others may be calculated from those already known. Some of the parameters in grinding is needed for calculation of the others parameter (Midha et al., 1991). Parts such as automobile, aerospace, and medical component are some examples of grinding machinability. Therefore, grinding is one of most important and most complicated aspects of tool production and poor grinding will results in poor parts performance (Badger, 2003).

Xie and Huang (2008) has stated that P20 steels are extensively used as structural materials in modern manufacturing industries due to their excellent properties, such as high hardness at both ambient and elevated temperatures, low thermal expansion, good wear resistance and chemical inertness. Grinding with aluminum oxide abrasives is the most commonly used machining process for the fabrication of structural components made of those P20 steels. However, the superior properties of the P20 steel materials also render the grinding extremely difficult. The cost associated with the grinding process has been a major factor that has hindered the applications of the AISI

P20 steel. As a consequence, in the past several decades great research efforts were directed towards the development of efficient grinding processes for AISI P20 steel (Xie and Huang, 2008). Since P20 steel is a hard metal, correct grinding technique will require to avoid grinding cracks and improve tool life.

The surface roughness, R_a is also an important factor affecting many manufacturing departments. The main objective to obtain the optimum parameter in grinding is to reduce as much as possible manufacturing time and cost. Since P20 steel is wide used in manufacturing industry, the lowest surface roughness, R_a and optimum parameter get from this study will reduce the finishing operation such as final polishing. Since grinding is mostly used as finishing method, which determines the functional properties of the surface, the knowledge of the surface quality and its control are crucial. It is therefore an effort to achieve high levels of surface quality; conditionally improved by the grinding process, choosing the appropriate cutting conditions. The quality of the ground surface is generally defined as the sum of the properties under consideration upon demands. It is a complex of system factors. Surface quality includes physical, chemical and geometric properties (Madl et al., 2003). The geometric surface properties include roughness parameters as a characteristic of micro geometry in the cut plane perpendicular to the surface.

Grinding fluids are used to cool the work piece and the grinding wheel. It is also used to transport debris away from the grinding zone, and to provide lubrication at the contact between the wheel and the work piece (Hryniewicz et al., 1998). In this study, water based ZnO Nano-coolant is used as a grinding fluid. The grinding fluid may significantly affect the condition at these interfaces by changing the contact temperature, normal and shear stresses and the distribution along the interfaces of the tool and work piece (Safian et al., 1990). In this study, a model has been developed to find the effect of grinding condition which is depth of cut, type of wheel and type of grinding fluid on the surface roughness and wheel wear.

1.2   Problem Statement

There are two major problem encounters in this study. First will be the cost of the operation. Improper finishing in grinding process will contribute to further machining process such as polishing. Therefore, the cost of operation will increase due to addition machining process. Besides that, the excessive temperature of the work piece during the grinding is one of the problem encounters in this study. There is an increase in the temperature of the work piece during the grinding process. The high temperatures generated in the grinding zone can cause some types of thermal damages to the work piece, for example burning, excessive tempering of the superficial layer with possible re-hardening and increase of the brittleness (Malkin, 1989).

1.3   Objective Of The Study

The objectives of these studies are to identify:

- To determine the effect of variation axial depth and types of wheel on the grinding surface quality.
- To determine the effect of Water Based Coolant and Nano-coolant on the grinding surface quality and wheel wear.
- To develop an artificial intelligent model using Neural Network for prediction modelling.

1.4   Scope of Study

The major scope of this study is the work piece material. P20 tool steel is used as a work piece to conduct my experimental study. Besides that, in this study, the work table speed is one the parameter which maintain in the constant rate throughout this experimental study which is at 200 rpm. Furthermore, this experimental study is conducted with a single pass and also multi pass. For the multi pass, four passes are conducted for each experiment. Equally important, is the range of the grinding depth in this study. The experiment conducted with grinding depth in the range of 5 to 21 µm. Besides, Aluminum Oxide wheel and Silicon Carbide wheel are used to grind the work

piece in this experimental study. Finally, the wheel dressing condition is similar after each of the experiments conducted.

1.5   Thesis Outline

This thesis contains five chapters which is every chapter have its own purpose. After viewing the entire chapter in this thesis hopefully viewer can understand the whole system design for this project.

Chapter one contains of the introduction or the overview of this project, the problem statement of this project, the objectives of the project, the scopes of the project and the outline of this thesis for every chapter.

Chapter two contains all the literature review. This chapter will explain the information about the article that related to the project that is done by other research. This chapter also describes the journals and other important information regarding this project.

Chapter three is a chapter for the methodology of this project. This chapter will explain about the detail of the project. It also includes the project progress that has blocked diagram, flowchart and also the explanation in detail about the project.

Chapter four discusses the result and the analysis for this project. This chapter will explain on the results and analysis of the project. The analysis includes the comparable results between project using water based coolant and Nano coolant. Both values will be compared to justify the theory.

Chapter five will explain the conclusion of the project. It also includes the future recommendation of the project.

CHAPTER 2

LITERATURE REVIEW

2.1   Introduction

According to Samek et al. (2011) grinding is the finishing machining operation to ensure the final surface quality. Compared with the operation methods of defined tool geometry, a tool for grinding consists of a number of statistically oriented grinding grains of random shapes. During the grinding process, small chips are removed along with high rates of material removal. Therefore grinding operations are used for machining difficult-to and hardened materials. The resulting surface quality depends on input factors such as principally cutting conditions are, followed by grinding material and accompanying phenomena. Generally, materials hard to machine are ground with finer grit wheels and a soft material are ground by coarse grained wheels. Cutting speed strongly influences the selection of a suitable grinding wheel degree. It is known that the higher cutting speed is, the finer the grinding wheel should be. The choice of optimal cutting conditions for grinding is not as strongly influenced by the requirement of keeping the optimum tool life, as is the case with other machining methods. Since grinding is mostly used as finishing method, which determines the functional properties of the surface, the knowledge of the surface quality and its control are crucial. It is therefore an effort to achieve high levels of surface quality, conditionally improved by the grinding process, choosing the appropriate cutting conditions. The quality of grinded surface is generally defined as the sum of the properties under consideration upon demands. It is a complex of system factors. Surface quality includes physical, chemical and geometric properties. The geometric surface properties include roughness parameters as a characteristic of micro geometry in the cut plane perpendicular to the surface (Samek et al., 2011).

2.2   Theory of Grinding

2.2.1   Mechanics of the Grinding Process

In the grinding process, the kinematic relationship between the grinding wheel and the work piece motions applies to each cutting grain. Some aspects of the process by which a grain grind can be illustrated by the geometrical relationship between a grain and the work piece during the grinding process. The geometry of the undeformed chip is shown in Figure 2.1
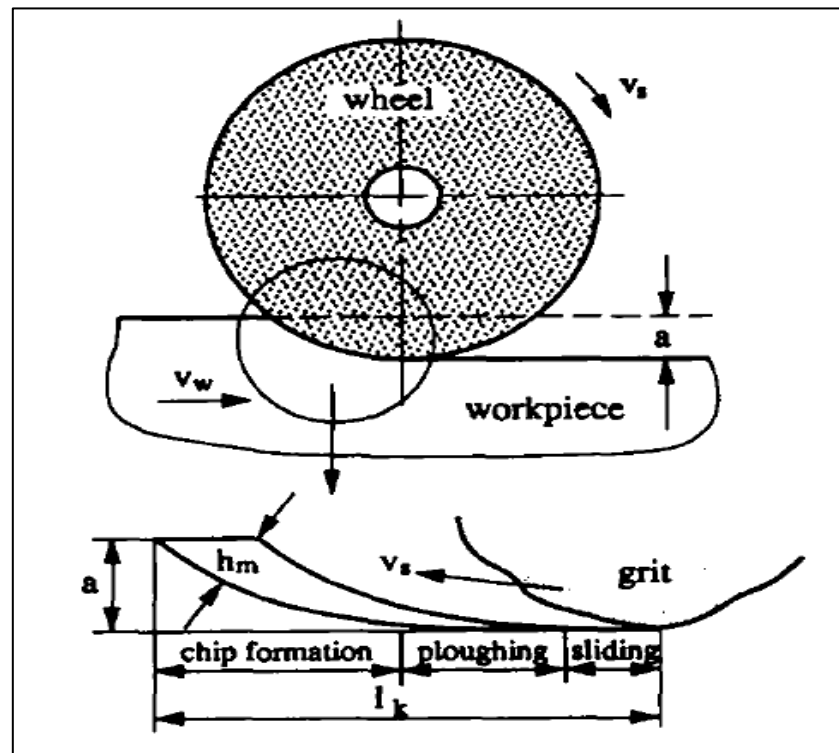
Figure 2.1: Three stages of chip generation

Source: Chen and Rowe (1995)

Based on the Figure 2.1 the undeformed chip shape is characterized by the cutting path length of the grain and the maximum undeformed chip thickness hm. The grinding process can be distinguished into three phases, including rubbing, ploughing and cutting. When the grain engages with the work piece up-cut grinding, the grain

slides without cutting on the work piece surface due to the elastic deformation of the system. This is the rubbing phase. As the stress between the grain and work piece increases beyond the elastic limit, plastic deformation occurs. This is the ploughing phase. The work piece material is piled up to the front and to the sides of the grain to form a groove. A chip is formed when the work piece material can no longer withstand the tearing stress. The chip formation stage is the cutting phase. From the point of view of the energy required to remove material, cutting is the most efficient phase. Rubbing and ploughing is inefficient, since the energy is wasted in deformation and friction with a negligible contribution to material removal. Furthermore a high temperature may result, producing an excessive rate of wheel wear and the work piece surface may suffer metallurgical damage (Chen and Rowe, 1995).

2.2.2   Thermal Analysis of Grinding

Malkin and Gou (2007) stated that the grinding process requires high energy expenditure per unit volume of material removed. Virtually all of this energy is dissipated as heat at the grinding zone where the wheel interacts with the work piece. This leads to the generation of high temperatures which can cause various types of thermal damage to the work piece, such as burning, metallurgical phase transformations, softening (tempering) of the surface layer with possible re-hardening, unfavourable residual tensile stresses, cracks, and reduced fatigue strength of the work piece.. Thermal damage is one of the main factors which affects work piece quality and limits the production rates which can be achieved by grinding, so it is especially important to understand the underlying factors which affect the grinding temperatures.

In earlier research in 1950, it was conclusively shown that most grinding damage is thermal in origin. The first attempt to correlate actual grinding temperatures with structural metallurgical changes in the work piece was reported five years later. For this purpose, an embedded thermocouple was used to measure temperatures in the work piece subsurface during grinding of a hardened bearing steel. Numerous other methods have also been developed to measure grinding temperatures using either thermocouples or radiation sensors. While considerable difficulties may arise in interpreting such measurements due to the extreme temperature gradients in time and space near to the

surface, embedded thermocouples and infrared radiation sensors utilizing fibre optics have been shown to provide a reasonably good indication of the work piece temperature near the ground surface. Both of these temperature-measuring techniques have been found to give results which are consistent with each other, and also with measurements of the surface temperature using a thin foil thermocouple.

Besides that, Malkin and Gou (2007) also mention that, temperatures are generated during grinding as a consequence of the energy expended in the process. In general, the energy or power consumption is an uncontrolled output of the grinding process. Temperature measuring methods do not provide a practical means to identify and control grinding temperatures in a production environment, as their use is generally restricted to the laboratory. In-process monitoring of the grinding power, when coupled with a thermal analysis of the grinding process, can provide a much more feasible approach to estimating grinding temperatures and controlling thermal damage. Thermal analyses of grinding processes are usually based upon the application of moving heat source theory. For this purpose, the grinding zone is modelled as a source of heat which moves along the surface of the work piece. All the grinding energy expended is considered to be converted to heat at the grinding zone where the wheel interacts with the work piece. A critical parameter needed for calculating the temperature response is the energy partition to the work piece, which is the fraction of the total grinding energy transported to the work piece as heat at the grinding zone. The energy partition depends on the type of grinding, the wheel and work piece materials, and the operating conditions (Malkin and Gou, 2007).

2.3   Analysis of Grinding Wheel Surfaces

2.3.1   Grinding Wheel

In grinding wheels, the cutting edges produced from the abrasive grains are arranged in a random fashion. Randomly arranged grains produce, in turn, a surface which profile could be considered as random. Raman et al. (2002) detailed the study of grinding wheel surfaces and have been reported on the measurement and analysis of the working surface of grinding wheels. Since the grinding wheel has a high surface speed

compared with the work piece surface, the surface of the grinding wheel which contributes to the cutting could well be taken as the effective profiles of the wheel comprising all the high points on the individual sections of the wheel. Attempts have been made to obtain this effective profile by superimposing individual section profiles, but it is an elaborate and time consuming approach (Raman et al., 2002).

2.3.2   Wheel Dressing Process

Vickerstaff (1975) have shown that a grinding wheel produces features on the work piece surface which can be directly attributed to the wheel dressing process. The traverse rate and shape of the single-point dressing diamond is particularly important.

Pahlitzsch (1954) suggest that the diamond actually cuts through the abrasive grit to produce what is effectively a form tool. The dimensions of this form are determined by the combination of diamond traverse rate, shape and in the feed. When the wheel is used for grinding the abrasive grits transfer their profile to the work piece surface.

Bhateja et al. (1972) recorded both wheel and work piece profiles by stylus measurement. Dressing features clearly appeared on the work piece surface, but could not be detected on the surface of the wheel. They suggest that this is probably because any grooves produced in the grid by the dressing process would be very small compared to the total roughness of the wheel.

According to Malkin and Cook (1971) the wheel was dressed with a single-point pyramidal diamond and the debris collected on grease covered glass slide. After dissolving away the grease and the metal chips the dressing particles were sieved and weighed to determine their size distribution. The original grit size and the wheel hardness were found to influence the size distribution of the dressing particles. Generally smaller grits and harder wheels gave smaller dressing particles. More significantly however, the dressing particles for all the wheels used were not much smaller than the grits which went into the wheels, indicating that the dressing diamond

actually fractures grits to' produce relatively large fragments or, possibly, dislodges them from the bond.

2.4   Grinding Parameter

2.4.1   Grinding Wheel Life

A wheel life model is developed in terms of the Group Method of Data Handling (GMDH) for studies of identification and prediction problems in complex systems in which wheel speed, feed, depth of cut, grain size, grade and hardness of work material are taken into consideration. In this method an accurate model of wheel life is obtained with the factors affecting it is chosen from a small number of input and output data. A mathematical model for grinding wheel redress life is identified by the polynomial theory of complex systems. Wheel speed, feed, grain size and grade are chosen as the independent variables from among the factors considered having an effect on wheel wear through the identification of the model. The model obtained enables the redress life to be predicted for all combinations of grinding wheel, work material and grinding conditions, and serves as an aid in the optimization of the grinding process (Nagasaka et al., 1979).

2.4.2   Surface Roughness on Work Piece

A grinding wheel has roughness in the axial and circumferential directions. The grinding grits flake, chip and fracture as well as is pulled out of the binder. Furthermore, when materials lying to high adhesion are ground the grit is capped by adherent lumps. The roughness of the wheel therefore changes continuously with the length and the number of passes.

The magnitude of the roughness is influenced by the hardness of the material ground as well as the elastic properties of the work piece, grit and binder materials. The elastic deflection of the grid at contact is generally found to be small.

Besides that, Vengkatesh et al. (1998) also proposed that another contributor to surface roughness which has received rather less attention than attrition and grinding mechanics is the wear and surface damage. The issue of wear has been addressed primarily for materials prone to high adhesion. The chemical and metallurgical mechanism of adhesion of metal to grit has been studied with a view to look at the blunting and attrition of the wheel. In terms of surface damage it has been suggested that the adhered material acts as a tool of large nose radius to tear and plough out large grooves on the surface. Grinding is a process which transmits power and generates traction. We are of the opinion that it is important to treat the rubbing regime in the contact zone of grinding as a general tribosystem which transmits traction by sliding or rolling and therefore may give rise to a variety of modes of metal removal. Such modes including the one by plastic grooving, collectively contribute to the generation of surface roughness. These modes are clearly sensitive to material properties such as hardness, toughness and fatigue strength, the operative values of which being dependent on the strain, strain rate and temperature generated in the contact zone. As stated in above, the localization of heat influenced by the thermal conductivity of material is a factor which is likely to affect wear and surface roughness. Under 'no wear' conditions material hardness is the primary factor which influences roughness. Under more severe operating conditions when the generated strain, strain rate and temperatures are high wear modes influenced by thermo-physical and fracture properties as well as microstructural stability under these conditions, come into play and add to the 'no wear' roughness. In this paper they have addressed the issue of material response to grinding, in generating surface roughness. We neglect attrition which has an interactive relation to material response by undertaking single pass operations only. Examinations of the wheel after single pass showed minimal attrition and after each roughness due to workpiece wear generated in surface grinding of metals pass the wheel is dressed afresh.

Vengkatesh et al. (1998) commence the study by recording the roughness generated under conditions of very low depth of cut from a variety of materials possessing a range of hardness. The analytical method used is power spectral analysis. The depth of cut is increased to generate conditions where the grinding force and traction also increase commensurately and wear and surface damage ensue. Using the 'no wear' roughness power spectrum generated by the method described in a previous

paper as a datum, we study the shift in this power spectra due to such damage as a function of depth of cut and material response. Grinding is done on the flats of aluminium, copper, titanium and a hard steel.

2.5   Grinding Fluid

2.5.1   Effectiveness of Grinding Fluid

The benefits of cutting fluids are generally recognized throughout the industry. Despite this, cutting fluids are often treated as an afterthought and given insufficient attention. Ebbrell et al. (1999) found that the boundary layer of air around the grinding wheel deflects most of the grinding fluid away from the grinding zone. A better understanding is required of the hydrodynamics of cutting fluid delivery and ways to optimize it.

A cutting fluid has three main functions when applied to the grinding process. There are, bulk cooling of the work piece, the flushing away of the chips and dislodged wheel grits and lubrication. Bulk cooling and flushing are reasonably understood but the lubrication effects of the cutting fluid are less clear. It is generally accepted that cutting fluids lower the grinding zone temperature due to lubrication, which reduces wheel dullest, rather than by removing heat from the grinding zone. By reducing wheel dulling, friction and hence power is reduced so that the heat generated is limited. Bulk cooling and flushing can be achieved even though very little fluid enters the contact region between the grinding wheel and work piece. Lubrication depends on fluid entering the contact region and although a large volume may not be necessary to achieve this purpose, fluid delivery will be ineffective if no fluid enters the grinding zone. This investigation was aimed at achieving a better understanding of the effect the boundary layer has on fluid delivery (Ebbrell et al., 1999).

2.5.2   Cutting Fluid Delivery

With regard to the grinding process particular problems exist due to the high surface speeds of the wheel, which causes a boundary layer of air around the wheel

periphery. The boundary layer restricts the flow of cutting fluid into the grinding zone. In example, flood delivery via a shoe or jet delivery tangential to the wheel via a nozzle, are not believed to fully penetrate this boundary layer and, thus, the majority of the cutting fluid is deflected away from the grinding zone. According to Ebbrell at el., flood delivery of a cutting fluid is usually delivered from a shoe which is fitted around the wheel surface. This method typically delivers large volumes of cutting fluid at low velocity. Therefore, earlier it was suggested this method was ineffective, especially under high speed grinding conditions where the energy of the fluid is not sufficient to penetrate the boundary layer of air surrounding the wheel. Delivery of cutting fluid via a nozzle in the form of a jet can have two benefits. Firstly the fluid can be delivered with a velocity great enough to penetrate the boundary layer of air and secondly, if applied at a high enough velocity, it may be used to clean the wheel mechanically by removing adhered metal.

The angle at which the cutting fluid is delivered has been the subject of much research in recent years. Delivering the cutting fluid as near to tangential to the grinding wheel as possible, is a common approach with the cutting fluid directed straight towards the grinding zone. However, this is contrary to investigations which have suggested the nozzle be positioned at an angle to the wheel periphery (Ebbrell et al., 1999).

Unfortunately different investigations have offered conflicting optimum angles at which to position the nozzle. This disparity may be due to the viscosity of the cutting fluid and its velocity at the nozzle exit. As stated by Trmal and Kaliszer (1976) the benefits of using scraper plates. Using a pitot tube to measure the velocity of the boundary layer, a decrease in air velocity occurred as the scraper plate was moved towards the wheel periphery. This is supported by Campbell who investigated the hydrodynamic pressure at the wheel or work piece interface caused by the passage of cutting fluid beneath the wheel. At a critical wheel speed this pressure measured zero Introducing a scraper plate allowed the grinding wheel speed to be increased by 20 % before the hydrodynamic pressure again measured zero. The need for high fluid velocities to penetrate the air boundary layer make the application of water based cutting fluids much more difficult in terms of a coherent jet.

2.5.3   Behavior of Cutting Fluid in the Grinding Zone

Fluid flow under a grinding wheel has come under investigation due to an attempt to determine the 'useful flow rate'. According to Ebbrell et al. (1999) useful flow rate is the quantity of cutting fluid which passes through the grinding zone and affects the grinding mechanism. A theoretical study by Guo and Malkin (1976) based on experimental results, concluded that the usefulness flow rate equaled the amount of fluid retained in the grinding wheel pores from the point of application to the point where grinding commences. A theoretical model for fluid flow through a porous medium was proposed based on experimental results. Conventional methods of fluid delivery tend to supply high volumes of cutting fluid of which only a small percentage may be considered as useful flow rate (Ebbrell et al., 1999).

Previous research investigated the film thickness of the cutting fluid in the micro gap of the contact area between wheel and work piece. Two cutting fluid delivery methods were considered where either the fluid is carried by adhesion on the wheel periphery into the grinding zone or the fluid is directed towards the wheel or work piece interface and enters the grinding zone. For the first delivery method where the cutting fluid is directed at some angle to the wheel periphery and the boundary layer of air carries the cutting fluid into the grinding zone, the maximum film thickness was estimated to be 40 µm. Delivering the same volume of fluid at the same velocity but with the nozzle positioned so that the cutting fluid was directed straight towards the grinding zone a film thickness of 80 µm was estimated. To fully optimize the process a method of delivery needs to be established where as much cutting fluid as possible passes through the grinding zone. Realistically losses of some degree will always occur, however, a greater understanding of the process may allow through-flow to be increased (Akiyama et al., 1984).

2.6   Behavior of P20 Steel

The work piece material is made of P20 steel which is widely used as a material for injection moulds. The P20 tool steels, known also as low carbon mild steel, contain chromium as a principal alloying element and it is known to have high resistance to

softening at elevated temperature. P20 is usually heat treated by austenitizing at 860 ◦C followed by oil quenching and tempering at 540 ◦C. A typical quenched and tempered P20 steel microstructure consists of a spherodized carbide particles in a, stress relieved, martensite matrix. The melting point of P20 steel (carbon content of about 0.42 at. %), determined from Fe–C phase diagram, is approximately 1490–1520 ◦C. However, due to the presence of other alloying elements, the given value for the melting point may vary slightly (Farhat, 2003). Since P20 steel is a hard metal, correct grinding technique will required to avoid grinding cracks and improve tool life, In this study, the cutting force produced when grinding P20 steel is investigated using response surface method (Hamdib et al., 2006).

2.7   Nano-Coolant

2.7.1   Introduction of Nano-Coolant

Nano-coolant is a new class of fluids engineered by dispersing nanometer-size solid particles into base fluids such as water, ethylene glycol, engine oil, cutting fluids and so on. In earlier research has shown that the thermal conductivity and the convection heat transfer coefficient of the fluid can be largely enhanced by the suspended nanoparticles. Recently, tribology research shows that lubricating oils with nanoparticle additives exhibit improved load-carrying capacity, anti-wear and friction reduction. These features make the Nano-fluid very attractive in some cooling or lubricating application in many industries including manufacturing, transportation, energy, and electronics (Shen, 2008).

2.7.2   Nano-Coolant for Cooling Application

Heat transfer fluids play an important role for cooling applications in many industries including manufacturing, transportation, energy, and electronics. According to Shen (2008) developments in new technologies such as highly integrated microelectronic devices, higher power output engines, and reduction in applied cutting fluids continuously increase the thermal loads, which require advances in cooling capacity. Therefore, there is an urgent need for new and innovative heat transfer fluids

to achieve better cooling performance. Generally, conventional heat transfer fluids have poor heat transfer properties compared to solids. As shown in Table 2.1, most solids have orders of magnitude larger thermal conductivities than those of conventional heat transfer fluids. Therefore, fluids containing suspended solid particles are expected to display significant enhancement in thermal conductivities relative to conventional heat transfer fluids. Numerous theoretical and experimental studies of the effective thermal conductivity of fluids containing particles have been conducted since Maxwell's theoretical work was published more than 100 years ago. However, these studies were confined to dispersions containing millimeter- or micrometer-sized particles. In developing advanced fluids for industrial applications, it was identified that millimeter or micrometer-sized sized particles have severe clogging and abrasive problems. With the development of Nano powder synthesizing techniques, it was proposed that nanometer sized solid particles can be uniformly and stably suspended in industrial heat transfer fluids such as water, ethylene glycol, or engine oil to produce a new class of engineered fluids with high thermal conductivity (Shen, 2008).

Table 2.1: Thermal Conductivity of Matters

Material	Thermal conductivity (W/m-K) at 300K
Metallic solids	
Copper	401
Aluminum	237
Titanium	22
Nonmetallic solids	
Diamond	2300
Silicon	148
Aluminum Oxide	36
Conventional heat transfer fluids	
Water	0.613
Ethylene Glycol	0.252
Engine Oil	0.145

Source: Incropera and DeWitt (2008)

2.7.3   Heat Transfer in Grinding

The grinding process generates an extremely high input of energy per unit volume of material removed. Virtually all this energy is converted to heat, which can cause high temperatures and thermal damage to the work piece such as work piece burn, phase transformations, undesirable residual tensile stresses, cracks, reduced fatigue strength, and thermal distortion and inaccuracies (Malkin, 1989). Numerous studies have been reported on both the theoretical and experimental aspects of heat transfer in grinding. Early research concentrated on predicting work piece surface temperatures in dry grinding in the absence of significant convective heat transfer (Outwater and Shaw, 1952). Subsequent investigations have provided a detailed understanding of heat transfer to the work piece, abrasive grains, grinding fluid, and the chips (DesRuisseaux and Zerkle, 1970). Thermal models have been developed to estimate the work piece surface temperature, heat flux distribution in the grinding zone, fraction of energy entering the work piece, and convective heat transfer coefficient for cooling on the work piece surface. Experimental investigations of heat transfer in grinding require accurate temperature measurements. Methods for temperature measurement in grinding include thermal imaging (Shen, 2008).

2.8   Reviews on Previous Article

2.8.1   Review on Wheel Wear

Pande and Lal (1975) have conducted an experiment on wheel wear in dry grinding surface. The result of their study shows that the wheel wear is increase together with increasing of volume of material removal rate. They have use two method to detect the wheel wear in grinding machinability, which is from Figure 2.2 (a) measurements of wheel diameter and also from Figure 2.2 (b) abrasive grains collected from the debris. Figure 2.2 shows the graph of volume of wheel wear versus volume of material removed. The wheel wear is increased when the volume of material removed from the work piece.
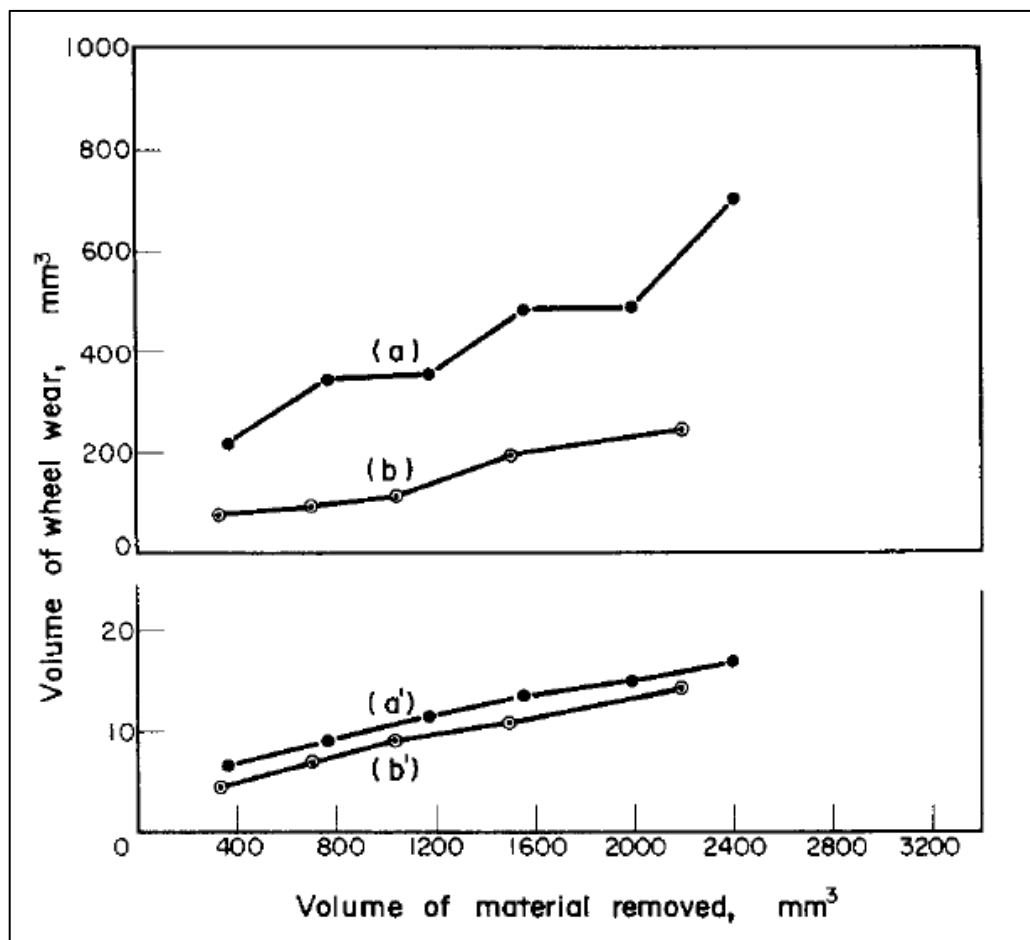
Figure 2.2: Graph volume of wheel wear versus volume of material removed.

Source: Pande and Lal (1975)

From the Figure 2.2, the wheel wear reduction of wheel diameter gives very high values. Figure 2.2 also shows that different wheel have different wheel wear. Wheel A46 H5 V10 (a') has higher wheel wear compared to wheel A60 J5 V10 (b').

Halder et al. (1979) has discussed about the variation of wheel wear and force with the number of passes. Halder et al. (1979) has shown the typical curves of variation of wheel wear and forces with the number of passes are shown in Figure 2.3 and Figure 2.4 respectively
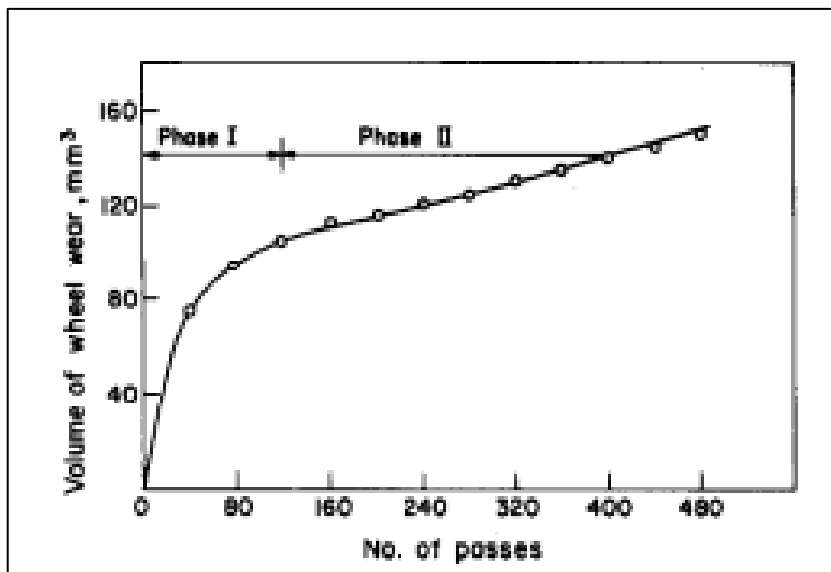
Figure 2.3: Variation of wheel wear with the number of passes.

Source: Halder et al. (1979)
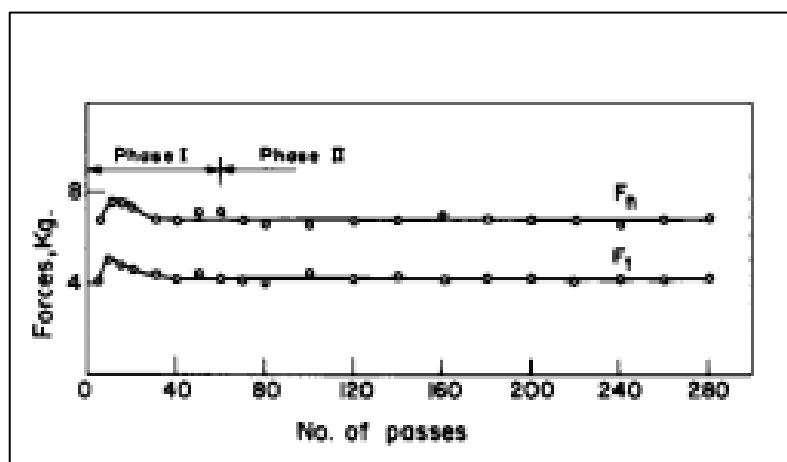
Figure 2.4: Variation of force with the number of passes.

Source: Halder et al. (1979)

The wheel wear was evaluated from the weight of wear particles collected during grinding. Phase I and phase II are clearly distinguishable. In phase II the wheel wear increases linearly whereas the forces remain more or less constant. Halder et al.

(1979) specified that the grinding ratio can be obtained from the slope of the curve in phase II.

Pande and Lal (1975) also conducted an experimental study on wheel wear on dry surface grinding. Figure 2.5 shows the experimental results which is the grinding ratio decreases with depth of cut. This indicated that the wheel wear increased with increase in depth of cut.
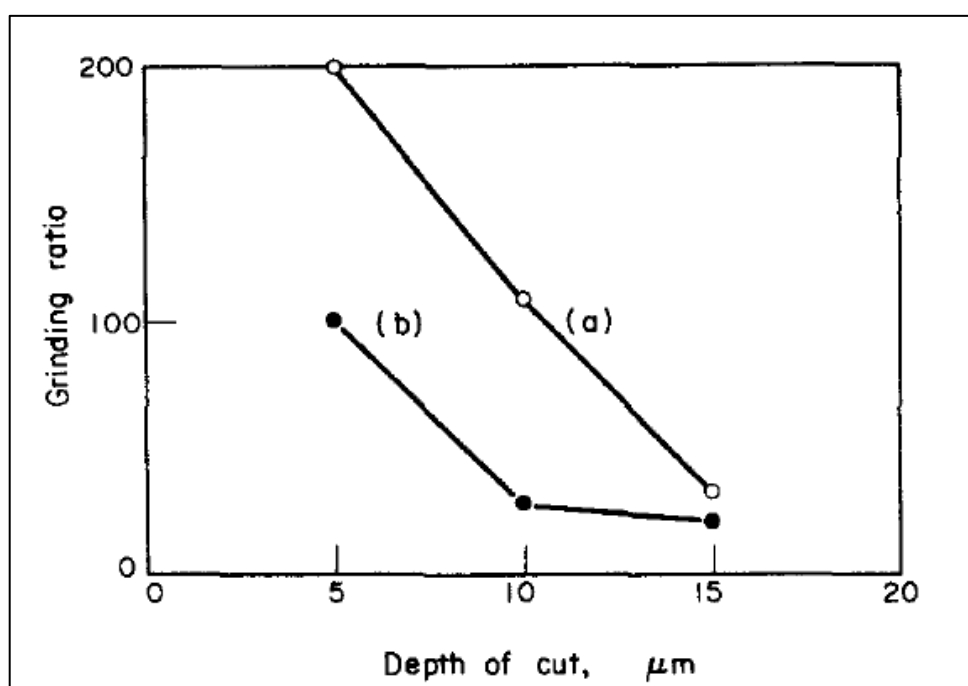
Figure 2.5: Variation of grinding ratio versus depth of cut.

Source: Pande and Lal (1975)

2.8.2   Review on Surface Roughness

According to Hecker and Liang (2003) the surface roughness model is based on the chip thickness model that includes many parameters such as: the wheel microstructure, the kinematic conditions, and the material properties. Therefore, the model can be used to predict the surface roughness under different conditions of these parameters. The depth

of cut and the speed ratio are the two most common kinematic variables set on the machine to obtain the desired grinding outputs. Figure 2.6 shows the surface roughness versus the depth of cut for three different speed ratios. It can be observed that variations on the depth of cut, in its lower range, produce significant changes on the value of the surface roughness. The model also predicts that at higher speed ratios the surface produced is smoother. This is because at a higher speed ratio that is at higher wheel velocity or lower work piece velocity, more grains participate in removing a given volume of material hence the depth of engagement is lower, producing smooth surfaces.
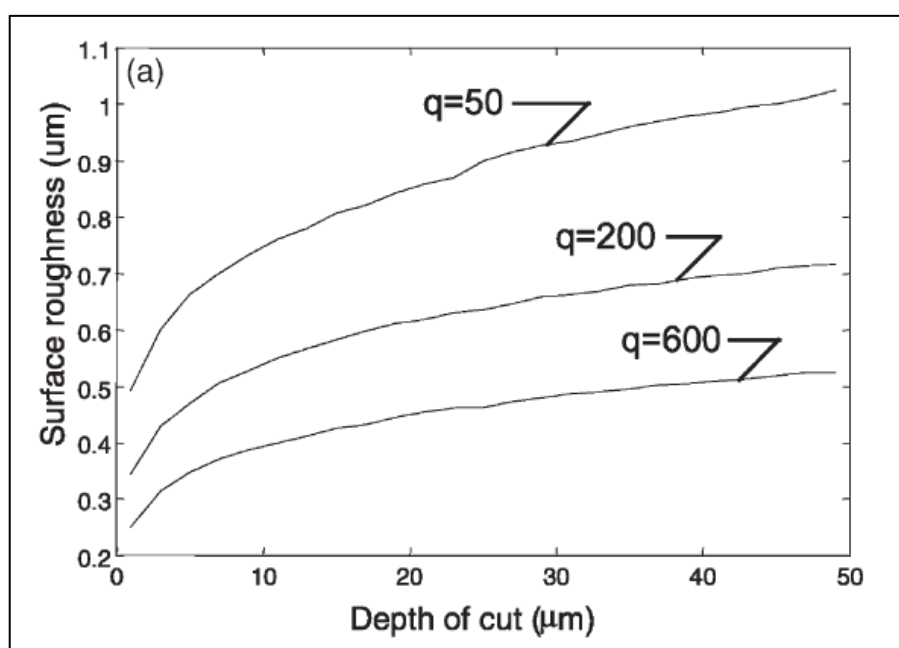
Figure 2.6: Surface roughness versus depth of cut for three different speed

Source: Hecker and Liang (2003)

Besides that, Hecker and Liang (2003) also mentioned that the wheel microstructure plays a major role in the quality of the ground surfaces. The wheel and dressing conditions used for the model calibration and validation were the same for each experiment.
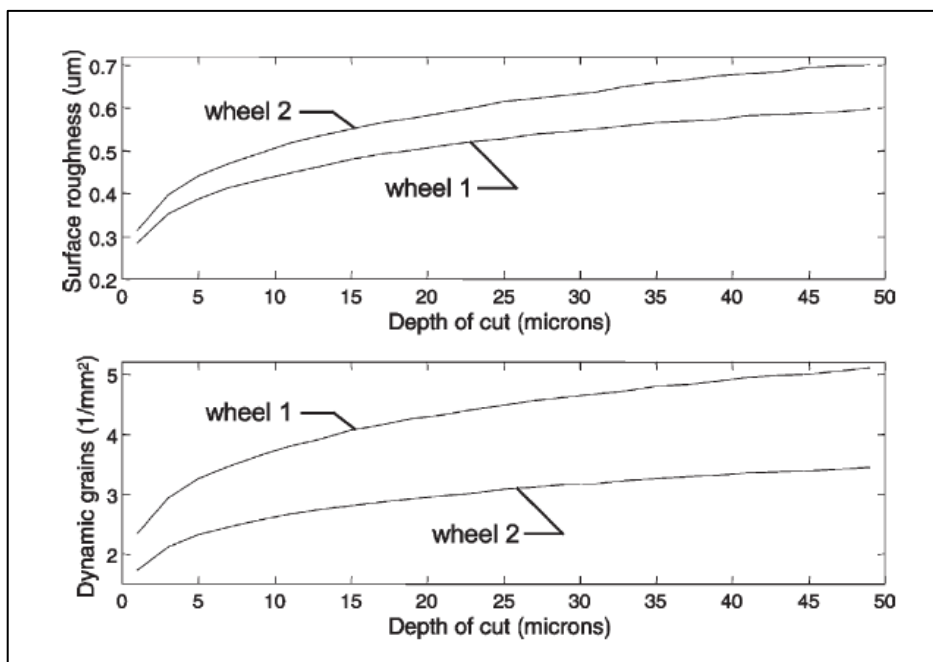
Figure 2.7: Surface roughness versus depth of cut for two different wheels.

Source: Hecker and Liang (2003)

Figure 2.7 shows surface roughness for two different grinding wheel which have different hardness. that As a result they found that a finer wheel produces better surface finish but it will cause higher forces and higher power due to the higher specific energy governed by a smaller expected value of the chip thickness (Hecker and Liang, 2003).

2.8.3 Review on Microstructure Imaging

Figure 2.7 and 2.8 shows the surface condition of nano-ZrO_2 ceramic after diamond grinding. The grinding condition is shown in Table 2.2. From the figure 2.7 there are a lot of abrasive dust on the finished surface. The grinding grooves are unequal in the width and depth. There are also a lot of plastic working marks and little brittle fracture on the surface after diamond grinding (Yanyan et al., 2008).

Table 2.2: Grinding Condition of nano-ZrO_2 Ceramic

Grinding Condition	
Work Table Speed	12 m/min
Wheel Speed	26.6 m/s
Depth of Cut	20 μm

Source: Yanyan et al. (2008)
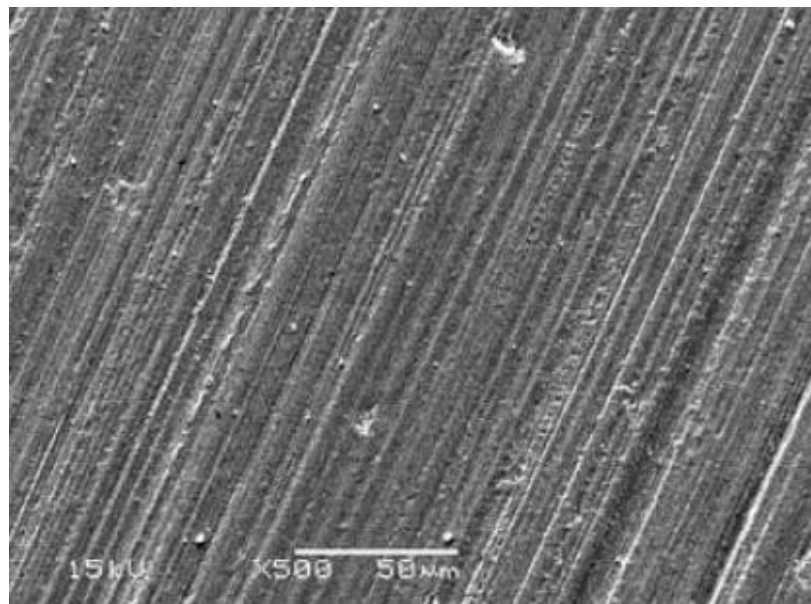
Figure 2.8: SEM photograph for 500 times magnification

Source: Yanyan et al. (2008)
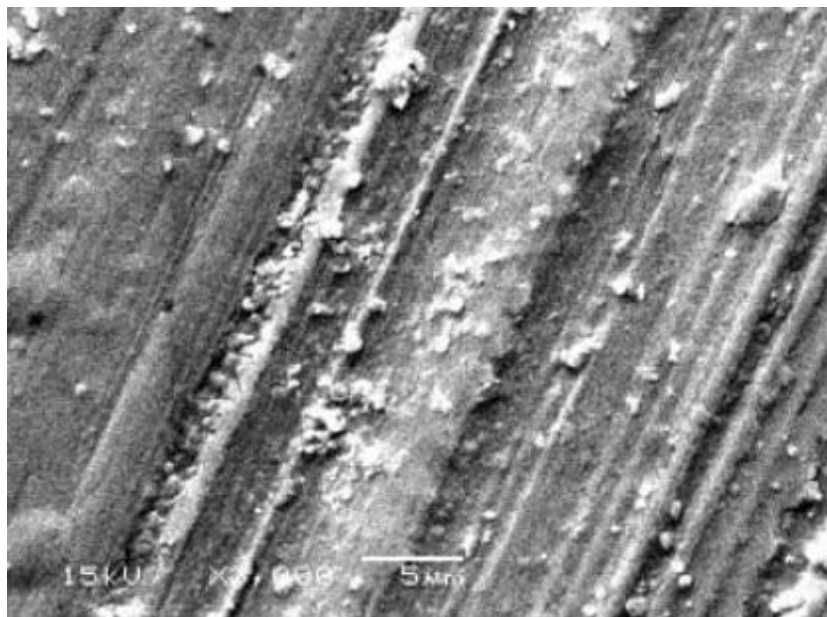
Figure 2.9: SEM photograph for 3000 times magnification

Source: Yanyan et al. (2008)

Figure 2.9 and 2.10 shows the surface condition of nano-ZrO_2 ceramic after diamond grinding. The grinding condition is shown in Table 2.3. From the figure 2.10 there are little abrasive dust on the finished surface. The grinding grooves are almost equal in the width and depth. There obvious plastic working but there is special machining mark found which is generated by the elliptical machining trace during grinding (Yanyan et al., 2008).

Table 2.3: Grinding Condition of nano-ZrO_2 Ceramic

Grinding Condition	
Work Table Speed	22 m/min
Wheel Speed	26.6 m/s
Depth of Cut	10 μm

Source: Yanyan et al. (2008)
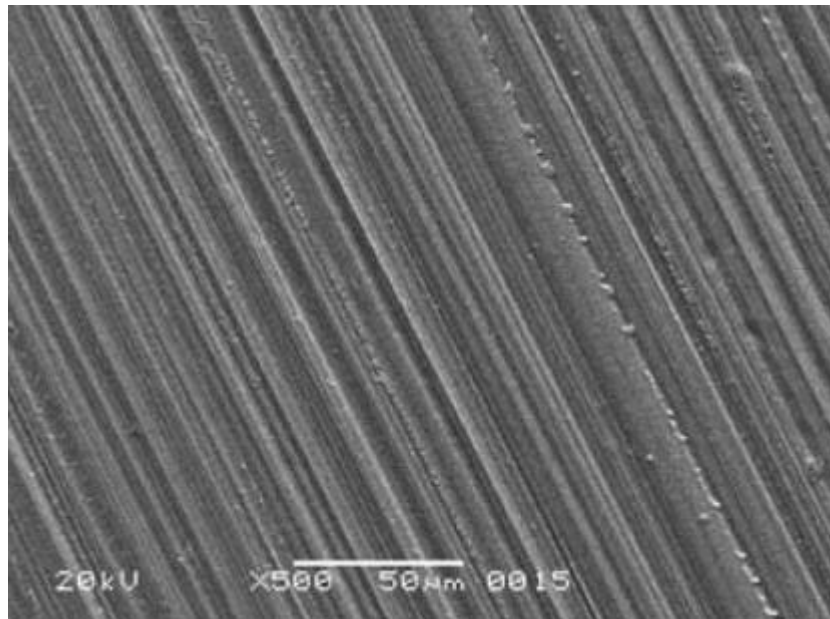
Figure 2.10: SEM photograph for 500 times magnification

Source: Yanyan et al. (2008)
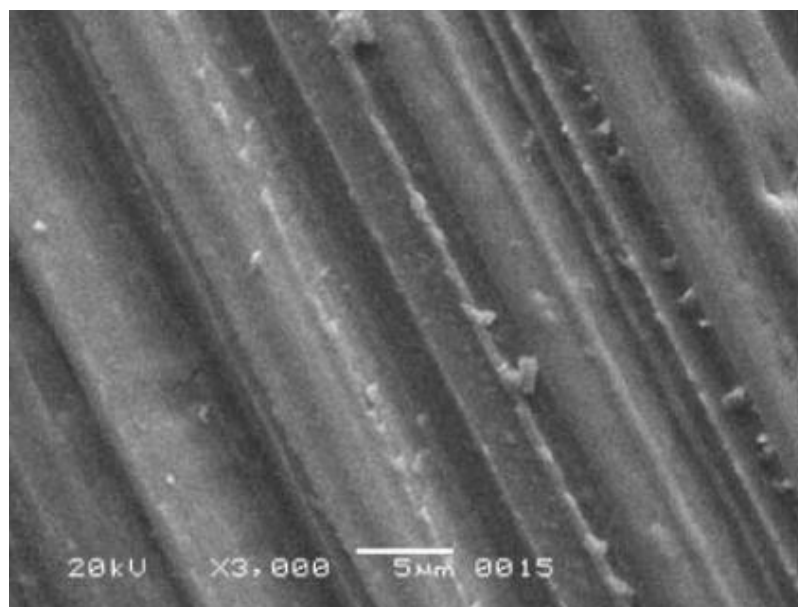
Figure 2.11: SEM photograph for 3000 times magnification

Source: Yanyan et al. (2008)

CHAPTER 3

METHODOLOGY

3.1   Introduction

This chapter will present the research methodology that had been used for the design the experiment of grinding machinability using AISI P20 tool steel. The main idea of this chapter is to describe all the steps that were used in this study. Based on the finding in chapter two, this chapter will emphasize all the process that had been carried out from the beginning of this chapter until the end of the research.

3.2   Work Piece Material

AISI P20 tool steel is used as work piece for this study. This material is in the category generally labelled as Mould Steels. Nickel and chromium are the alloying elements for hardness and toughness. The table below shows the chemical composition of AISI P20 tool steel.

Figure 3.1: P20 tool steel

Table 3.1: Chemical Composition of P20 Tool Steel

Composition	Weight percentage, %
Carbon	0.35-0.45
Silicon	0.2-0.4
Manganese	1.3-1.6
Chromium	1.8-2.1
Molybdenum	0.15-0.25

Source: Krishna et al., 2001

3.3   Preparation of ZnO Nano-Coolant

3.3.1 Preparation of Distil Water.

Aquamatic Water Still is used to produce the distilled water to dilute the ZnO nano-coolant. The produced distilled water will be collected in the huge container. Roughly around 27 *l* of distilled water need to be prepared for the nano-coolant dilution.

Figure 3.2: Aquamatic Water Still

3.3.2 Single Step Dilute Approach

Figure 3.3 shows the undiluted ZnO nano particle. The weight percentage of this undiluted nano particle is 50 % by weight and the density of undiluted ZnO nano particle is 5600 kg/m^3. Three bottles of ZnO nano particle are added together in beaker to find the volume. The volume of these three bottles is 180 l. Before the dilution process, 27 l of distilled water needed to be prepared in a pail. After that, slowly add the ZnO nano fluid together with the distilled water in the pail. The Eq. (3.1) shows conversion of weight percentage to volume percentage of ZnO nano fliud. From the Eq. (3.2) the total amount of distilled water to be added will nano particle can be obtained.
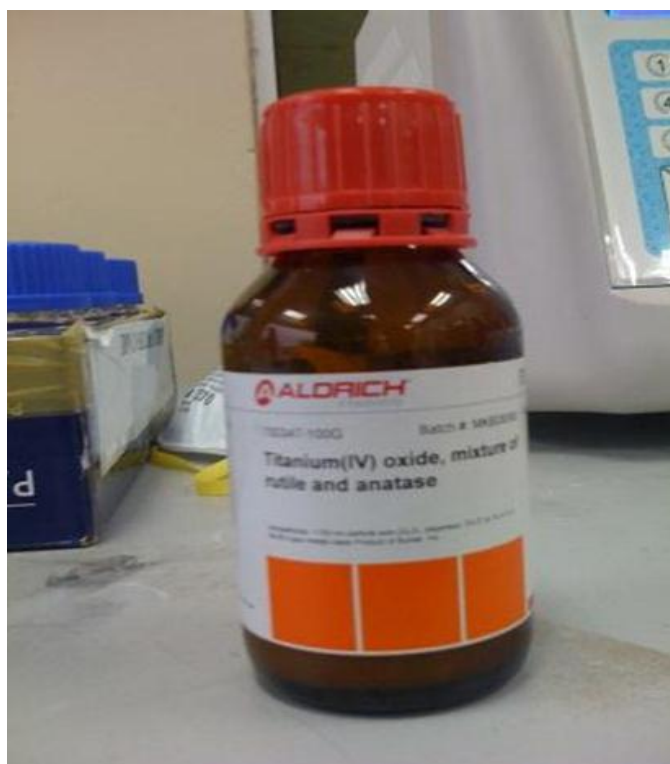
Figure 3.3: ZnO nano particle

From Eqn. (3.1) the weight % of ZnO nano particle has been converted to 0.1515 volume %.

$$\emptyset = \frac{\varphi\, \rho_w}{(1-\varphi)\rho_p + \varphi\rho_w} \tag{3.1}$$

$$= \frac{(0.5)(1000)}{(1-0.5)(5600)+(0.5)(1000)}$$

$$= 0.1515\ \%$$

Eqn. (3.2) shows that approximately 27.09 l of distilled water required to dilute the nano particle to become 0.1 concentrations of Zn0 nano-coolant. Finally, 0.1 concentrations of nano-coolant is used to grind the P20 tool steel work piece. For the 0.1 concentration of nano-coolant, the thermal conductivity, k will be 29 W/m-K and the specific heat, C_v will be 514 J/kgK.

$$\Delta V = V_1 \left(\frac{\emptyset_1}{\emptyset_2} - 1 \right) \tag{3.2}$$

$$= 180 \left(\frac{0.1515}{0.001} - 1 \right)$$

$$= 27090\ ml$$

3.3.3 Stirring and Observation Process

Motorize Stirrer is used to stir the diluted ZnO nano-coolant. The speed of the motor is set to 1000 rpm. This process will conduct for one hour. After the stirring process, the diluted ZnO nano-coolant will slowly poured into the huge bottle for observation process. The observation process will conducted for two weeks to make sure the diluted liquid is in stable state. If two layers of liquid are formed in these two weeks, then the diluted ZnO nano-coolant is unstable. Therefore, this procedure need to repeat again with different volume of nano fluid to form a stable state diluted ZnO nano-coolant. Figure 3.4 shows the stirring and observation process of nano-coolant.

Figure 3.4: Stirring Process using Motorize Stirrer

3.4   Grinding Process

3.4.1   Grinding Machine

.

Figure 3.5 shows the grinding machine which is used to grind the P20 tool steel. The grinding machine model is SUPERTEC STP-1022 ADC II. The work table speed for this grinding machine set to be constant. Besides that, the range of the cutting depth can adjust using digital system and also manually. Furthermore, magnetic system is used in this machine to hold the work piece while grinding operation. The flow rate of coolant has maximized throughout the experiment is conducted

Figure 3.5: Precision Surface Grinder

3.4.2   Measuring the Work Table Speed

The work table speed will maintain at a constant speed throughout this experimental study. Tachometer is used to measure the constant work table speed which is 200 rpm. Figure 3.6 shows the tachometers which used to calculate the constant work table speed of grinding machine.

Figure 3.6: Tachometer

3.4.3   Clamping System

Steel clamp is used to hold the work piece during the grinding process. This is because the magnetic system of the machine cannot hold the alloy material. Therefore steel clamp has been used to clamp the work piece. After clamping the work piece, the surface need to be checked and make sure it is flat. Figure 3.7 shows the steel clamp used to clamp the work piece during the grinding process.

Figure 3.7: Work piece clamped using a steel clamp

3.4.4 Grinding Wheel

There are two types of grinding wheel that have been used to conduct the experiment which is Silicon Carbide wheel and Aluminium Oxide wheel. Table 3.2 shows the properties of the grinding wheel.

Table 3.2: Properties of the Grinding Wheel

Properties	Silicon Carbide Wheel	Aluminum Oxide Wheel
Density, g/cm^3	3.1	3.67
Hardness, kg/mm	2800	2100
Thermal Conductivity, W/m·$^{\circ}$K	120	18

Source: www. http://accuratus.com/silicar.html

The diamond coated wheel dresser is used to dress the grinding wheel. Each after every experiment is conducted, the wheel dressing need to do. This is because the debris on the wheel will affect the experimental results. Figure 3.8 shows the diamond wheel dresser which is used to dress the Silicon Carbide wheel and the Aluminium Oxide wheel.

Figure 3.8: Single point wheel dresser

3.4.5 Surface Roughness Measuring

Pethometer is used to measure the surface roughness of the work piece. Total three measurements will take in each experiment which is in the two edges and also in the middle of the work piece. Finally the mean of the surface roughness is used to analysis the data. Figure 3.9 shows the Pethometer which is used to measure the surface roughness of the work piece after conducted each experiment.

Figure 3.9: Pethometer

3.4.6   Microstructure Imaging

Three different cutting depths from each experiment have been chosen for metallographic analysis using Scanning Electron Microscope (SEM). It consists of cutting depth of 5 µm, 11 µm and 21 µm. SEM is used to generate high-resolution images of shapes in the work piece after performing the grinding process. The microscope model is Carl Zeiss AG EVO 50 Series. Table 3.2 shows the specification of the microscope.

Table 3.3: Specification of SEM

Specification	
Magnification	**Field of View**
5 to 1,000,000 times	6mm at the Analytical Working Distance

Source: http://www.speciation.net/Database/Instruments/Carl-Zeiss-AG/EVO-50-
Series.html

3.4.7   Experimental Setup

Overall, the grinding experiment has been conducted by by using two different types of grinding coolant which is a water based coolant and ZnO Nanao-coolant. First, grinding process will be conducted using water based coolant for two different types of wheel which is SiC wheel and Al_2O_3 wheel. For the each type of wheel the grinding process will conducted for a single pass and multi pass. The grinding process will conduct with nine sets of experiment with different cutting depth. The cutting depths are 5 µm, 7 µm, 9 µm, 11 µm, 13 µm, 15 µm, 17 µm, 19 µm and 21 µm. Therefore, there will be total 36 experiment for water based coolant grinding. The experiment will continue with ZnO nano-coolant grinding. However there are only one wheel be used for ZnO nano-coolant grinding which is SiC wheel. But, the grinding methods are same as the water based coolant grinding experiment which is single pass and multi pass. The cutting depth also will be the same as water based coolant grinding. Therefore, there will be total 18 experiments for ZnO nano-coolant grinding experiment. The wheel

dressing will be done after each of the experiments using diamond coated wheel dresser. The surface roughness are measured after each of the experiment is conducted. Three different optimum cutting depth is chosen for SEM analysis which is 5 μm , 11 μm and 21 μm. The work piece has been cut into 3 cm × 3 cm for SEM analysis.

3.5   Data Modelling

3.5.1 Artificial Neural Network (ANN)

Artificial Neural Network (ANN) is used for modelling the data of surface roughness after generate the result of the grinding process. Data of each experiment will be converted to Microsoft Excel Coma Separated Value File type. This file will be opened in Neural Network Software. The software which used for modelling the data is Alyuda Neuro Intelligent. After import the data into this software, the data will be arranged in tanning, testing and validation mode as shown in Table 3.3. Depth of Cut will be selected as the input and Surface Roughness will be selected as output to modelling the results.

Table 3.4: Input and Output data

	(N) Depth of Cut	(N) Surface Roughness
TRN	5	0.446
TRN	7	0.467
TRN	9	0.689
TST	11	0.782
TRN	13	0.866
TRN	15	0.917
TRN	17	0.962
TRN	19	0.989
VLD	21	1.12

Next, will be the architecture design of the neurons. Two neurons and one hidden layer will be selected to design the network. Figure 3.10 shows the image of the network with two neurons and one hidden layer.
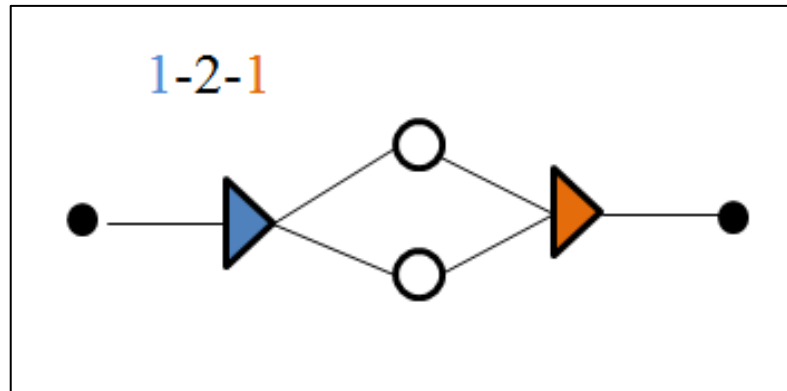
Figure 3.10: Image of Network

Following, the architecture design option will be changed. The method that will be used is Heuristic Search method. Then, the fitness criteria will be changed to R-squared and the iteration increased to 1000. Lastly, the automatically select the best network icon will be clicked. Next, the data will be trained. Regarding that, the network training option needs to be changed. Online back propagation will choose as a training algorithm. Then, the stop training condition will be by error value with the Mean Square Error (MSE) is 0.1×10^{-5}. Table 3.5 shows the network training option that will be used before training the data.

Table 3.5: Network Training Option

Network Training Option	Value
Training Algorithm	Online Back Propagation
Stop Training Condition	MSE

After the network trained, the data will be tested between the actual and output data. The correlation and the R-squared value must be higher than 85 %. Therefore the network will be trained until the correlation and the R-squared value higher than 85 %. After the network is tested, manual query is used to find the surface roughness for cutting depth between 21 µm to 50 µm. Finally, surface roughness versus cutting depth is plotted according the output of the network.

CHAPTER 4

RESULT AND DISCUSSION

4.1 Introduction

This chapter is important to investigate and to discuss about the results involve in this research. The analyses have been divided into Surface Roughness, Microstructure and Wheel Wear. The final part of this chapter was discussed about the prediction modelling using Artificial Neural Network.

4.2 Analysis on Surface Roughness

4.2.1 Single pass Experiment

Figure 4.1 shows the variation of surface roughness with different depth of cut for the single pass experiment. Generally, the trend of the Surface Roughness, R_a increases inconstantly when the depth of cut increases. First, the experiment which is conducted with water based coolant using Silicon Carbide wheel obtained the highest value of Surface Roughness, R_a which is 0.710 μm for cutting depth 5μm. However, the Surface Roughness, R_a increase inconstantly until 1.748 μm for cutting depth 21 μm.

On the other hand, the experiment which conducted with water based coolant with Aluminium Oxide wheel obtained Surface Roughness, R_a slightly lower than the first experiment. The Surface Roughness, R_a for 5 μm cutting depth is 0.622 μm and it is increasing inconstantly until 1.687 μm. But, the experiment conducted using Zinc Oxide nano-coolant obtained the lowest value of Surface Roughness, R_a which is 0.446 μm for cutting depth 5 μm and it is increased to 1.120 μm for cutting depth 21 μm. In general,

the measurements of surface roughness have shown an increase in magnitude as the depth of cut increases.

This is because the heat generated between the work piece and grinding tool zone will be higher for larger depth of cut. The high heat generated in this zone will contribute to the burning effect on the work piece. Therefore, the higher the axial depth of cut will contribute to higher Surface Roughness, R_a. (Krisha et al., 2008). Besides that, for lower cutting depth, more grains will participate in material removing hence the depth of engagement is lower and producing smooth surfaces. However, for higher cutting depth the grain that interacts with the work piece will perform the uniformed chip on the work piece surface which produces a rough surface. (Hecker and Liang, 2003) Hence, it shows that the Surface Roughness, R_a increases when the depth of cut increases in grinding machinability.

The experiment conducted using water based coolant with Aluminium Oxide wheel obtained lower Surface Roughness, R_a compares to experiments conducted with Silicon Carbide wheel. This is because of different hardness of the wheel. Refer to Table 3.2, Silicon Carbide wheel is much harder the Aluminium Oxide wheel. Therefore, when single pass experiment is conducted with Silicon Carbide wheel, first the grinding wheel will grind in the self-sharpening region where bond post fracture is predominant and later grinds in a zone of mixed conditions. For example, partly sharpening and partly blunting. In the final range blunting becomes predominant (Pande and Lal, 1975). This statement proves that the work piece grind using Silicon Carbide wheel will have high surface roughness comparable to Aluminium Oxide.

The experiment conducted using Zinc Oxide nano-coolant obtained the lowest Surface Roughness, R_a. This is because Zinc Oxide nano-coolant has high thermal conductivity compare to water based coolant. Therefore, nano-coolant has the capability to carry away the heat in the grinding zone (Saidur et al., 2010). Once the heat has been removed from the grinding zone, burning defect would not appear on the surface of the work piece. Therefore the Surface Roughness, R_a of the work piece will be much higher than the water based coolant.
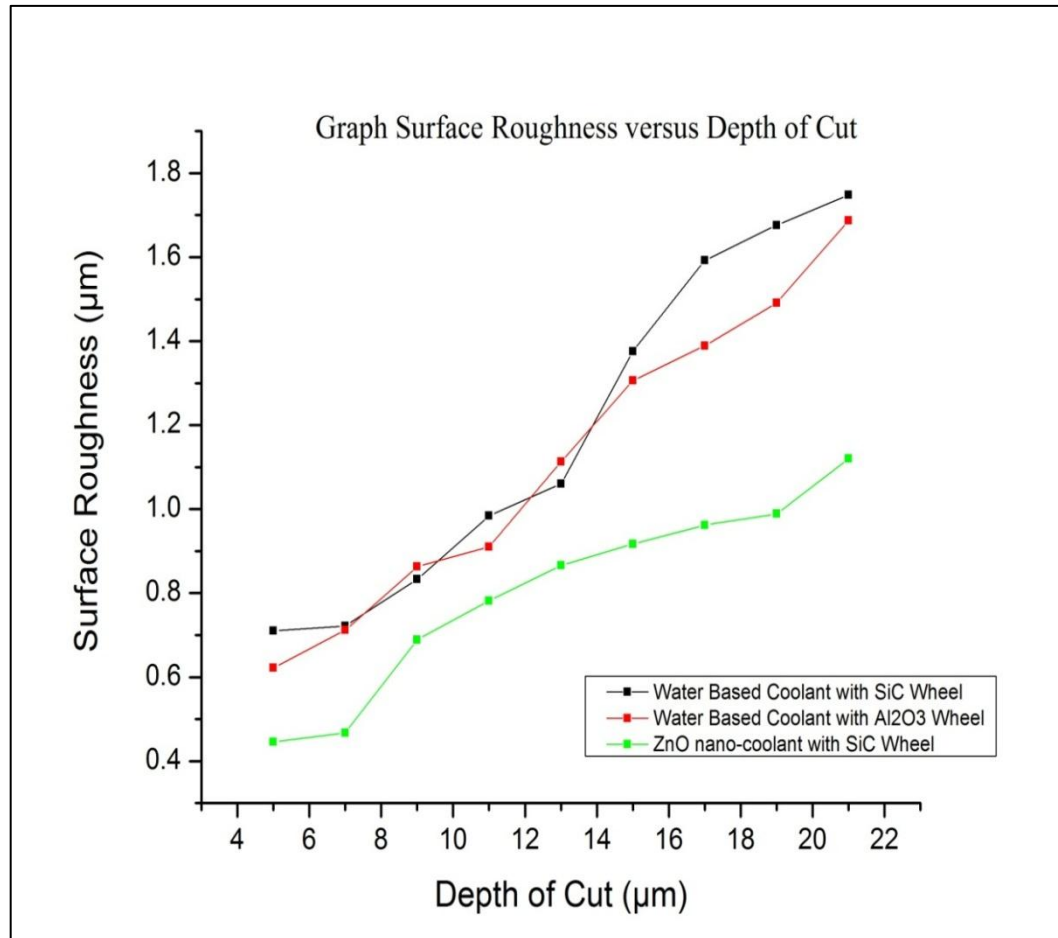
Figure 4.1: Graph Surface Roughness versus Depth of Cut for single pass grinding

4.2.2   Multi passes Experiment

Figure 4.2 shows the variation of surface roughness with different depth of cut for multi pass experiment. Generally, the trend of the Surface Roughness, R_a increases inconstantly when the depth of cut increases. First, the experiment which is conducted with water based coolant with SiC wheel obtained the highest value of Surface Roughness, R_a which is 0.570 μm for cutting depth 5 μm. However, the Surface Roughness, R_a increase inconstantly until 1.412 μm for cutting depth 21 μm.

On the other hand, the experiment which conducted with water based coolant with Al_2O_3 wheel obtained slightly lower than the first experiment. The Surface Roughness, R_a for 5 μm cutting depth is 0.529 μm and it is increasing inconstantly until 1.293 μm. But, the experiment conducted using ZnO nano-coolant obtained the lowest

value of Surface Roughness, R_a which is 0.225 μm for cutting depth 5 μm and it is increased to 0.541 μm for cutting depth 21 μm. As stated above, the reason for the trend of the graph for the multi pass experiment will be the similar as the single pass experiment.

However, the Surface Roughness, R_a result obtained for the multi pass experiment is lower than single pass experiment. This is because when the single pass grinding experiment is conducted on the surface of the work piece the grain engages with the work piece in an up-cut grinding, the grain slides without cutting on the work piece surface due to the elastic deformation of the system. But, in the multi pass grinding experiment the work piece material piles up to the front and to the sides of the grain to form a groove and complete chips have been performed (Chen and Rowe, 1995). Therefore, multi pass grinding experiment will obtain better Surface Roughness, R_a compared to single pass grinding experiment.
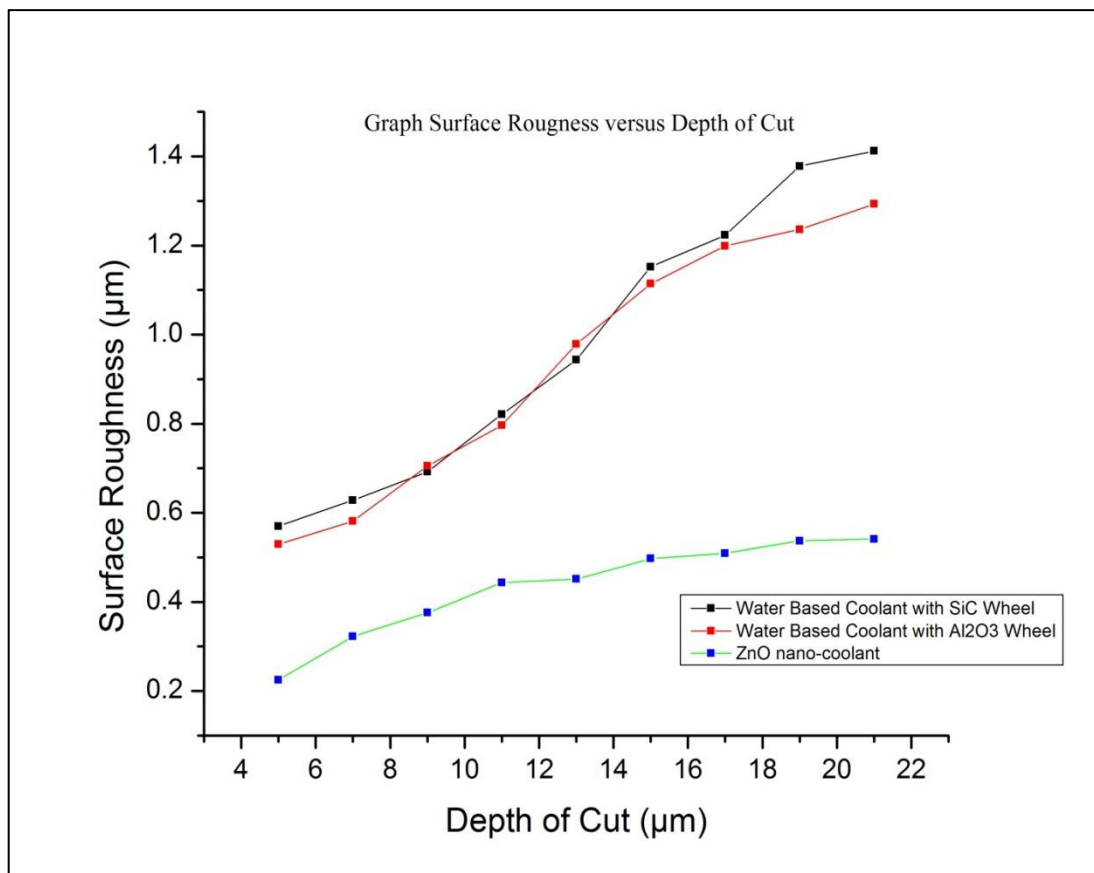
Figure 4.2: Graph Surface Roughness versus Depth of Cut for multi pass grinding

4.3 Metallographic Analysis

4.3.1 Metallographic Analysis for Water Based Coolant Grinding

Figure 4.3 and Figure 4.4 shows the SEM results for experiments conducted using water based coolant for cutting depth 5 µm. It is seen from Figure 4.3 and 4.4 there are little burning colour occur on the work piece surface. Beside that, there are also some continues smooth scratches produced on the grind surface. These scratches are produced by the interactions of abrasive cutting points with the work piece. Since, the interactions between the abrasive and the work piece are little for cutting depth 5µm therefore, the scratches are finer. On the other hand, the grinding grooves are almost the same in the width and depth. In the previous research, when the interface temperature is high enough, the work piece material at the contact zone becomes ductile enough to cause strong welds to form between the abrasive grit and work piece, thereby resulting in the generation of plastically deformed coatings (Xu et al., 2002). This statement supported the result when there is some burning colour scratches occur on the work piece surface.
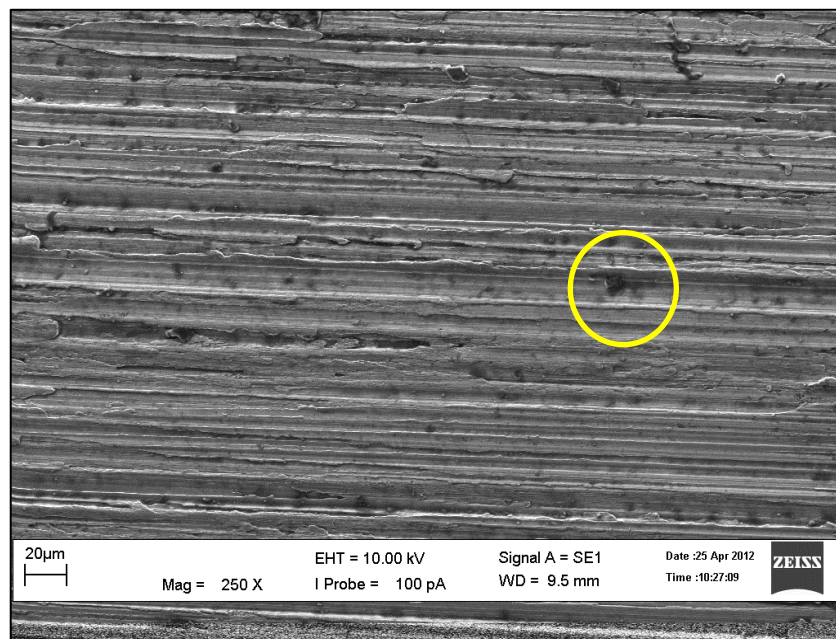
Figure 4.3: SEM result of cutting depth 5 µm with magnification 250 times
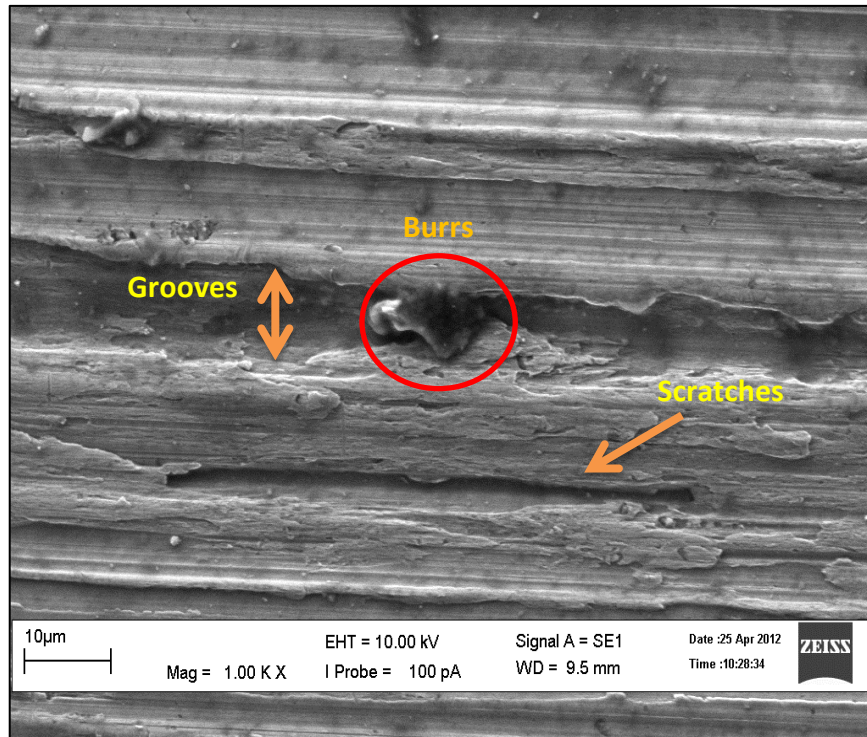
Figure 4.4: SEM result for cutting depth 5 µm with magnification 1000 times

Figure 4.5 and Figure 4.6 shows the SEM results for experiments conducted using water based coolant for cutting depth 11 µm. It is seen from Figure 4.5 and 4.6 there a lot of burning colour occur on the work piece surface compared to Figure 4.3 and Figure 4.4. If we observe the groove size, it is unequal in width and depth. Besides that, there are much more overlapped scratches produces compared to Figure 4.3 and Figure 4.4. This is because, when cutting depth is increased the the heat generated in the grinding zone will be higher. Therefore, the possibility of burning occur on the work piece surface is higher. As stated before, when the grinding interface temperature is high enough the work piece material at the contact zone becomes ductile enough to cause strong welds to form between the abrasive grit and work piece, thereby resulting in the generation of plastically deformed coatings (Xu et al., 2002).

Figure 4.5: SEM result for cutting depth 11 µm with magnification 250 times

Figure 4.6: SEM result for cutting depth 11 µm with magnification 1000 times

Figure 4.7 and Figure 4.8 shows the SEM results for experiments conducted using water based coolant for cutting depth 21 μm. It is seen from Figure 4.7 and 4.8 there a lot of huge burning colour occurs on the work piece surface compared to Figure 4.3 to Figure 4.6. Besides that, the scratches produce for cutting depth 21 μm are overlapping each other. Furthermore, the grooves are unequal and not continues. On the other hand, there are a lot of raising edges or small pieces of material remaining attached to a work piece which is called burrs on the surface. This contributes to the high value of surface roughness. This is happening due to the plastic deformation occur on the surface of the material in conjunction with the thermal effect (Davim, 2010). Besides that, the excessive heat peneterates into the work piece also contribute to the huge amount of burning on the work piece surface.

Figure 4.7: SEM result for cutting depth 21 μm with magnification 250 times

Figure 4.8: SEM result for cutting depth 11 µm with magnification 1000 times

4.3.2   Metallographic Analysis for ZnO Nano-coolant Grinding

Figure 4.9 and Figure 4.10 shows the SEM results for experiments conducted using ZnO nano-coolant for cutting depth 5 µm. It is seen from Figure 4.9 and 4.10 there are less burning colour occur on the work piece surface compared to Figure 4.3 to Figure 4.6. Besides that, the scratches produce for cutting depth 5 µm are very smooth compared to the Figure 4.3 to Figure 4.8. Furthermore, the grooves in the finished surface after grinding using ZnO nano-coolant are smoother, wider and also shallower than the material grind using water based coolant. Beside that, there is no burr occurred on this surface. This contributes to produce the finest surface roughness compared to the other experiment. This is due to the high thermal conductivity of ZnO nano-coolant which will absorb the heat that penetrate into the work piece during grinding. This phenomena cause the work piece material less burning effect and less plastic deformation occur when using ZnO nano-coolant compares to work piece which grind using water based coolant. On the other hand, ZnO nano-coolant having high viscosity which will reduce the sliding friction between the wheel and work piece (Prakash and Malshe, 2010). Reduce in the sliding friction produce the smooth grooves on the work piece surface as shows in Figure 4.9 and Figure 4.10.
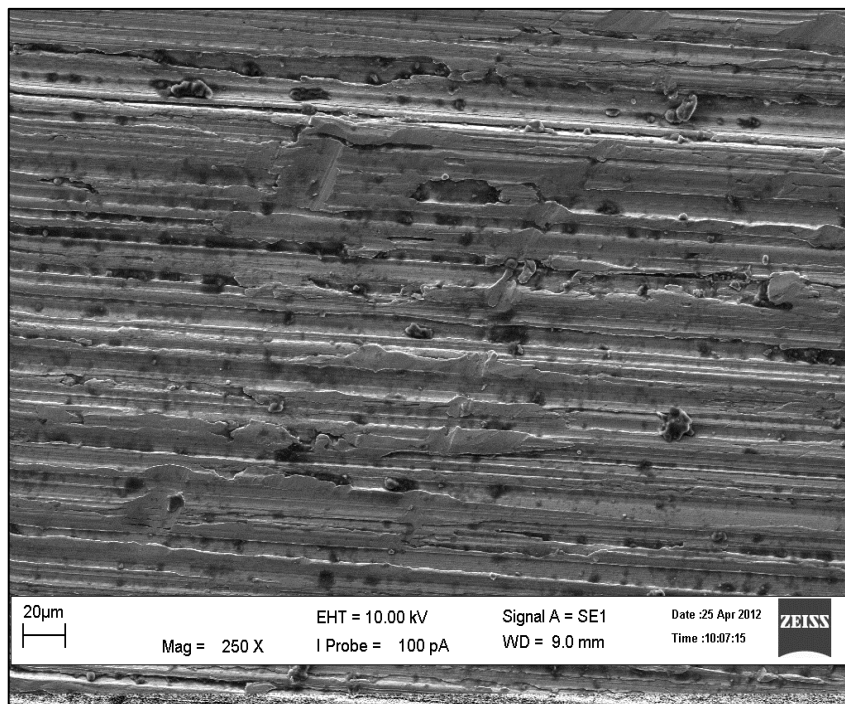
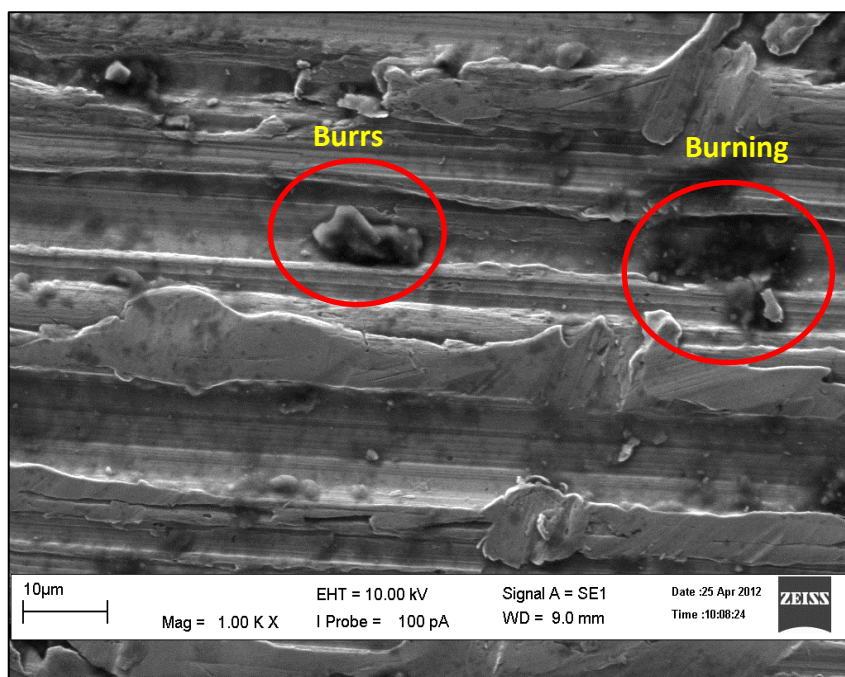**Figure 4.9**: SEM result for cutting depth 5 µm with magnification 250 times
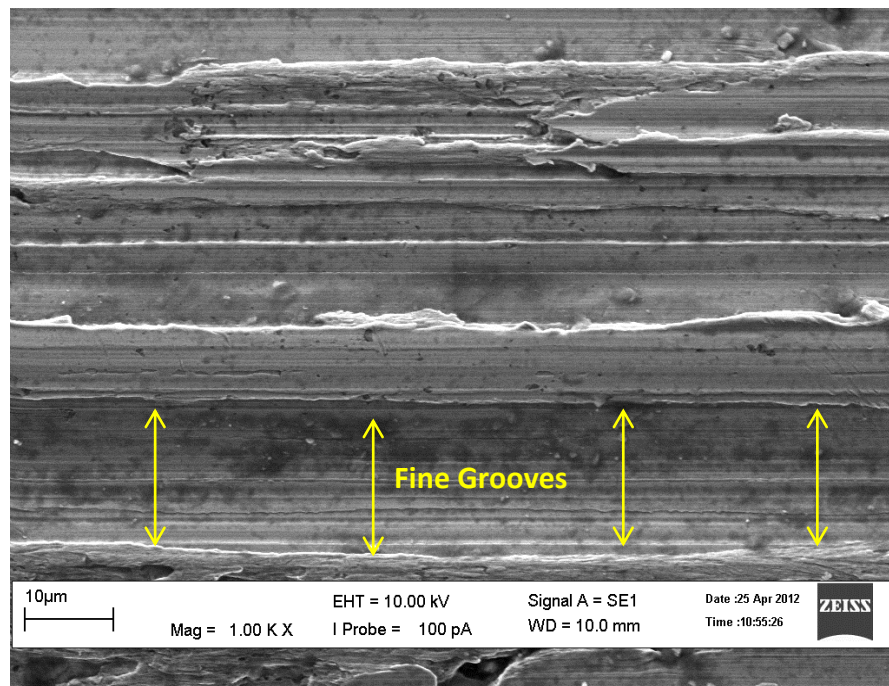
Figure 4.10: SEM result for cutting depth 5 µm with magnification 1000 times

Figure 4.11 and Figure 4.12 shows the SEM results for experiments conducted using ZnO nano-coolant for cutting depth 11 µm. The results show that the scratches produce for cutting depth 11 µm are rough compared to the Figure 4.9 and Figure 4.10. Moreover, the grooves produce for cutting depth 11 µm are inconsistent in size. There are some grooves are wide and deep. There are also some grooves very shallow. However, compare to Figure 4.5 and Figure 4.6 which using water based coolant for cutting depth 11 µm, this result produces much finer scratches and grooves. This is because the ZnO nano-coolant carry away the heat generates in the grinding zone (Saidur et al., 2010). Therefore, there are less plastic deformation occur on the material surface and produce a better surface roughness.
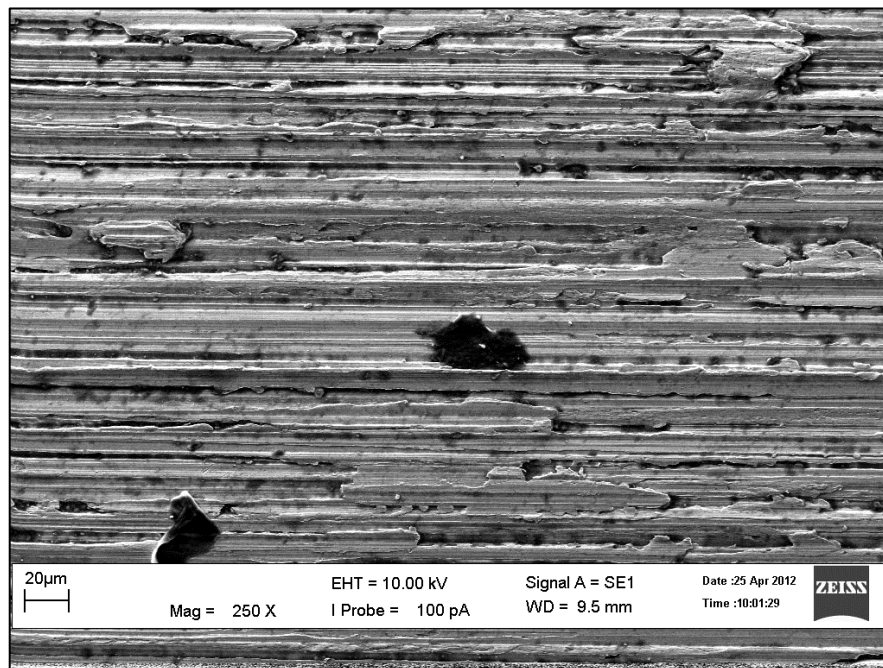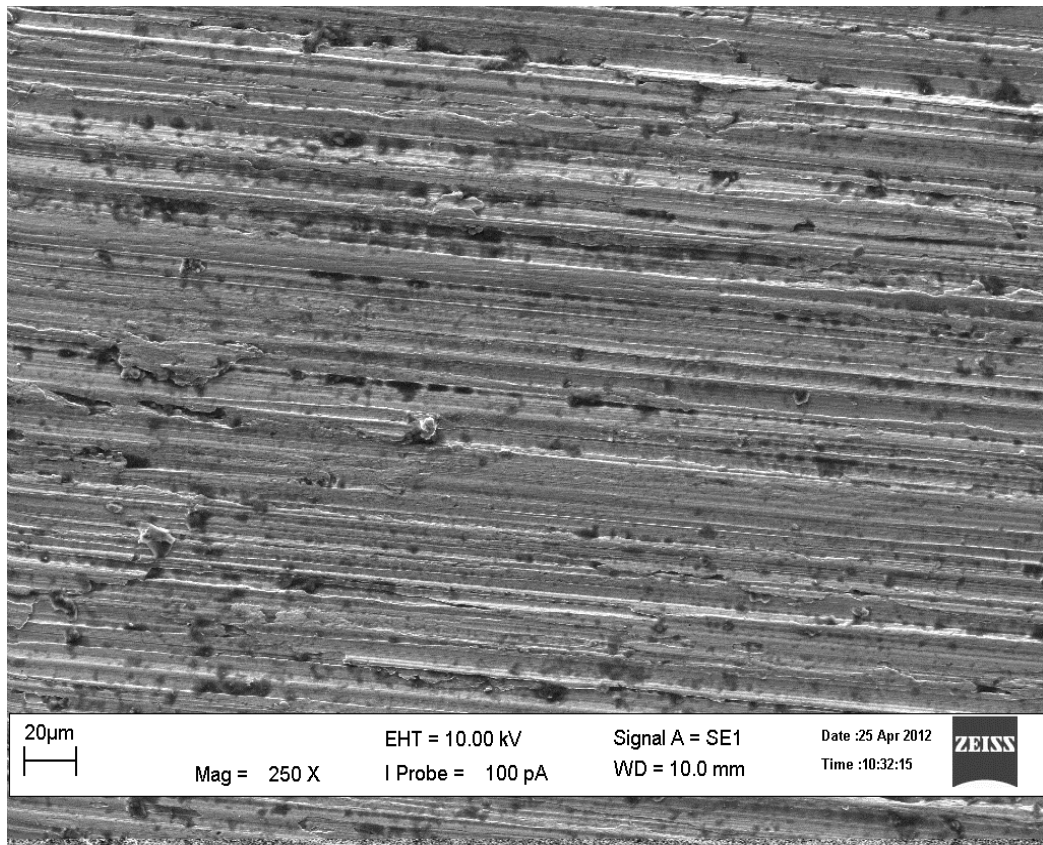

Figure 4.11: SEM result for cutting depth11 µm with magnification 250 times
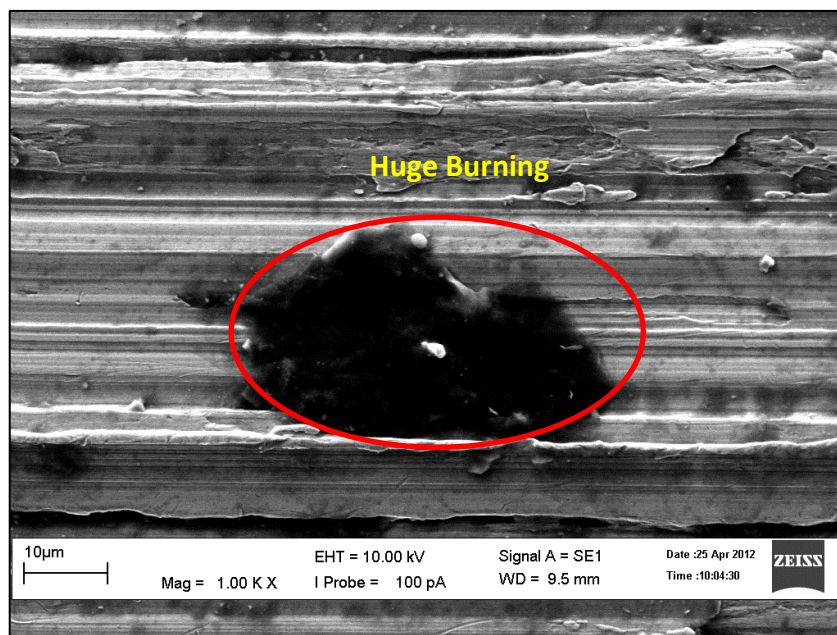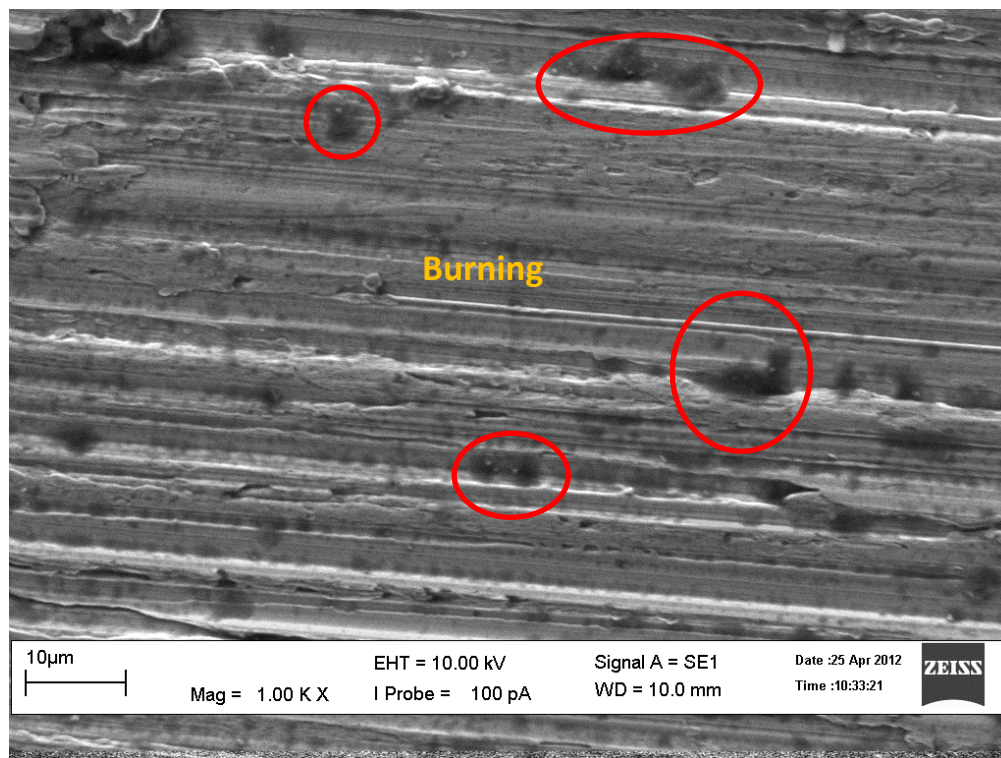
Figure 4.12: SEM result for cutting depth 11 μm with magnification 1000 times

Figure 4.13 and Figure 4.14 shows the SEM results for experiments conducted using ZnO nano-coolant for cutting depth 21 μm. The results show that the scratches produce for cutting depth 21 μm are very rough compared to the Figure 4.9 to Figure 4.12. In addition, the grooves are unequal and not continues. Beside that, there also some burning colour can be observed from the Figure 4.13 and Figure 4.14. But, the contain of burrs are fewer compared to Figure 4.13 and Figure 4.14. It shows that there is some improvement on the surface microstructure when grind using ZnO nano-coolant. As stated before this is due to the high thermal conductivity of nano-coolant. Nano particles tent to carry away the heat generates in the grinding zone (Saidur et al., 2010). However, the heat generates in grinding zone for cutting depth 21 μm are much higher than cutting depth 5 μm and 11 μm.
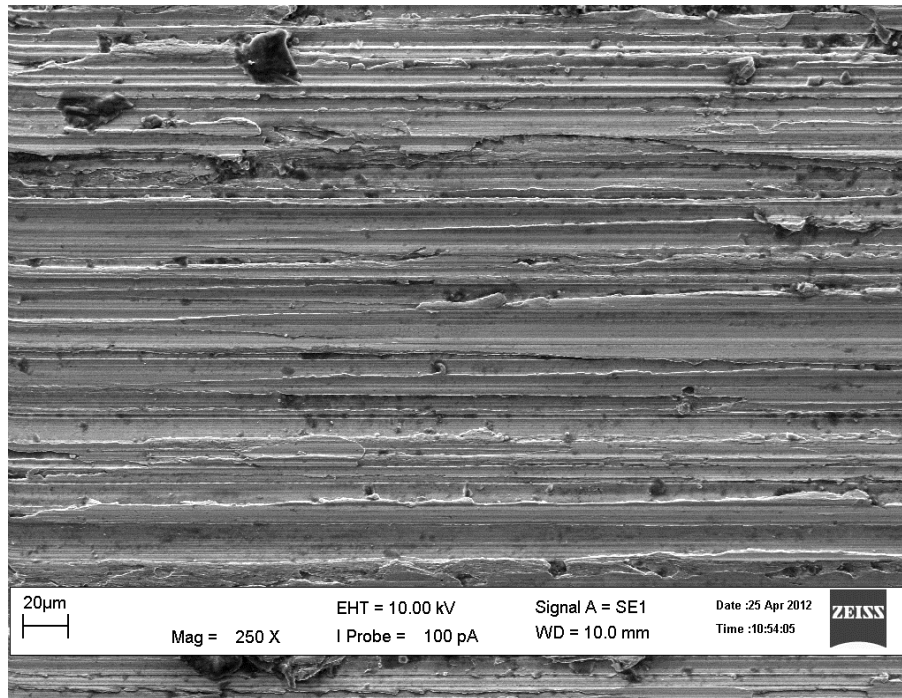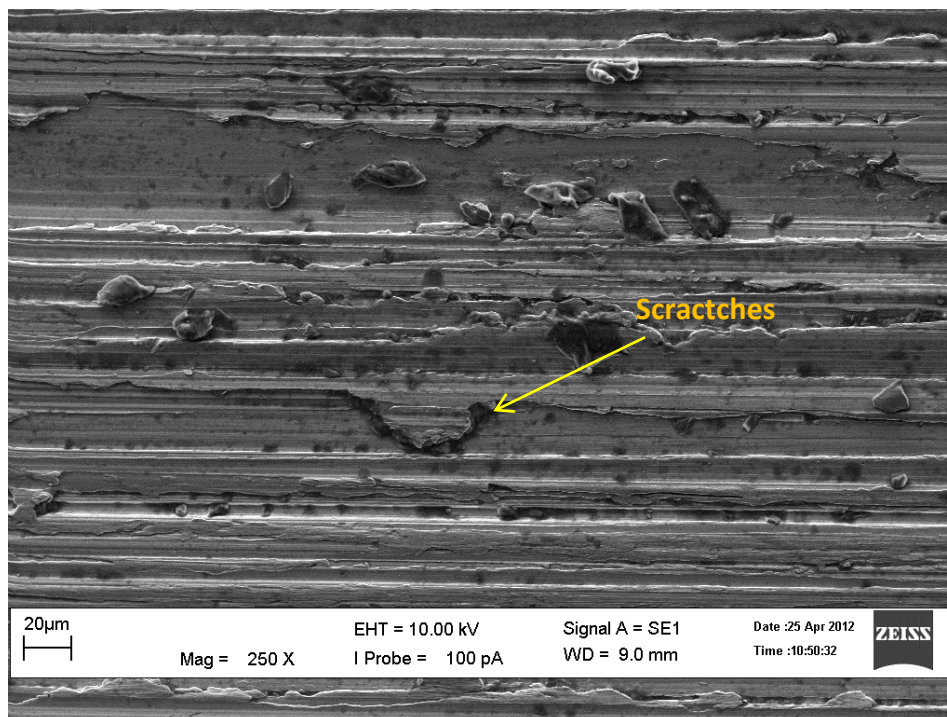
Figure 4.13: SEM result for cutting depth 21 µm with magnification 250 times
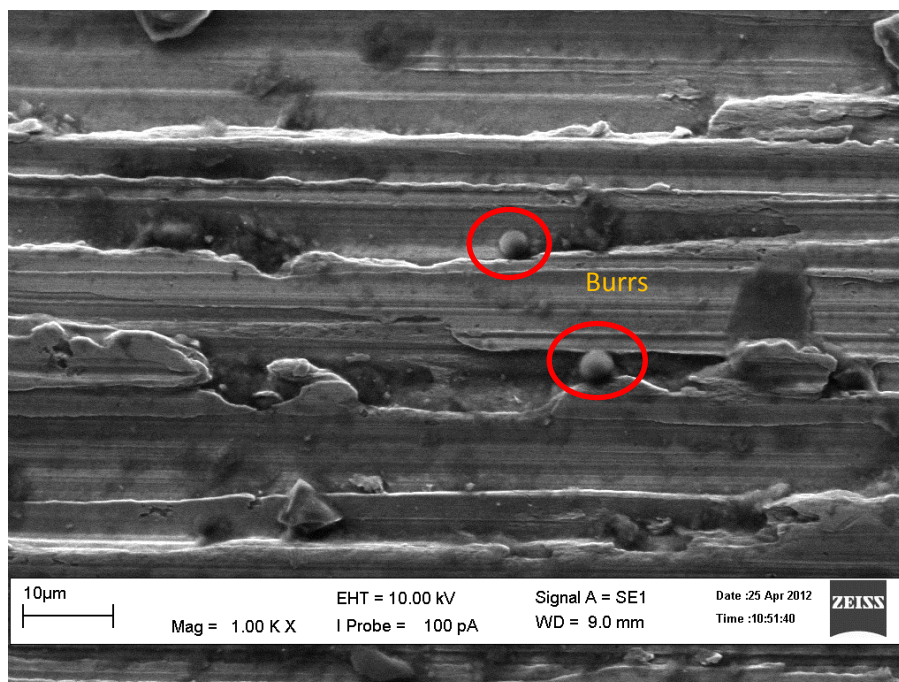
Figure 4.14: SEM result for cutting depth 21 µm with magnification 1000 times

4.4   Analysis on Wheel Wear

4.4.1   Wheel Wear for SiC Wheel Experiment

Figure 4.15 shows the variation of wheel wear with different depth of cut using Water Based Coolant and ZnO nano-coolant grinding. Generally, the graph trend of the Wheel Wear increases inconstantly when the depth of cut increases in water based coolant grinding. All the experiment did not obtain any wheel wear for cutting depth 5 μm. The multi pass grinding conducted using water based coolant having the highest wheel wear comparisons to other experiment which is increased to 0.10 mm for cutting depth 21 μm. However, the same experiment conducted with single pass grinding obtains slightly fewer from multi pass experiment. For cutting depth 21 μm, the wheel wear is 0.08 mm. Overall, the wheel wears increase when there is increase in cutting depth of grinding for Water Based coolant grinding.

This is because an increase in the depth of cut contributes a rapid increase in normal force on the grinding wheel. Therefore the wheel fails to remove all the metal the fed to it. Consequently, the down feed becomes interference and causes rapid increase of the normal force and grinding becomes progressively less efficient and increase the wheel wear (Pande and Lal, 1975). Besides that, Figure 4.15 also shows that experiments conducted using multi pass obtain higher value of wheel wear compared to experiments conducted with a single pass. This is because in a single pass grinding, there is only grain fracture occurs at the wheel but in multi pass there are bond fracture starts to occur which contribute to dulling the wheel and increases the wheel wear (Pande and Lal, 1975). These contribute to high wheel wear compare to single pass grinding for multi pass grinding. Figure 4.15 shows there is no significant chance in the wheel wear when experiment conducted using ZnO nano-coolant. This shows that ZnO nano-coolant is better protection and the wheel wear. This is due to the thin slurry layer on the wheel can protect the bonding material from thermal mechanical damage, thereby causing a low wheel wear which is insignificant (Shen et al., 2008).
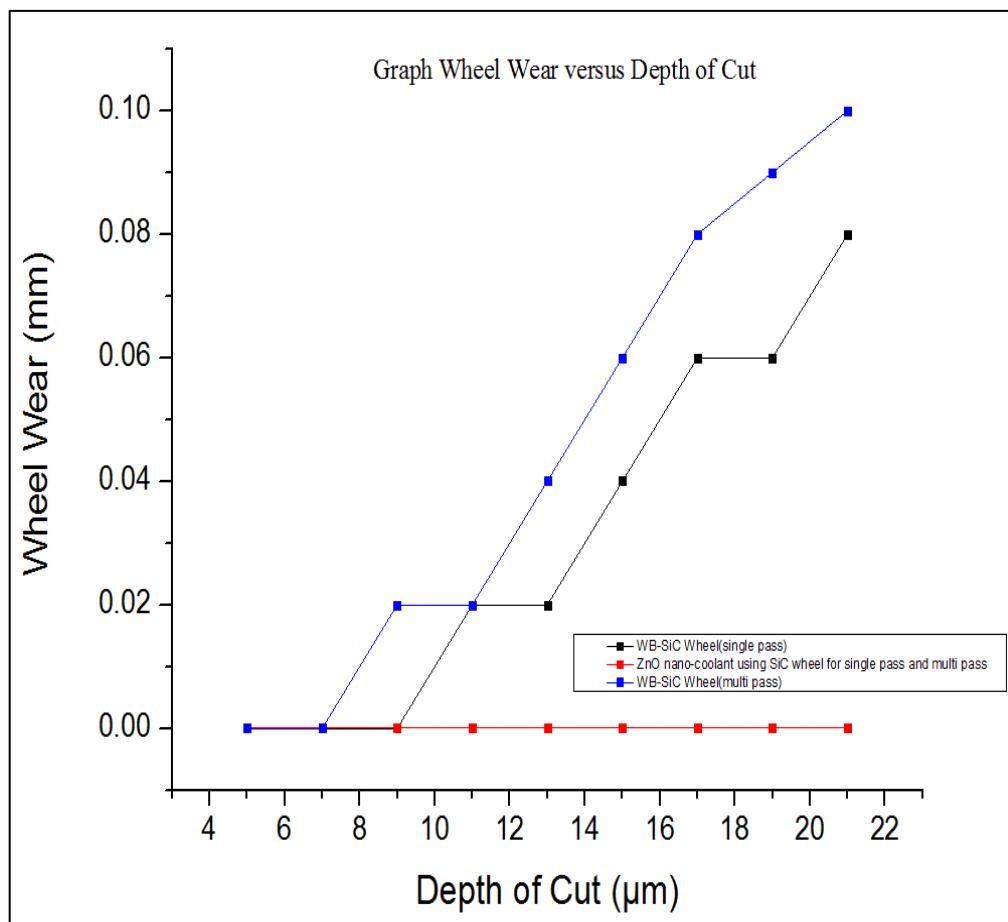
Figure 4.15: Graph Wheel Wear versus Depth of Cut for different coolant

4.5   Prediction Modeling of Artificial Neural Network (ANN)

4.5.1   Modeling on Single Pass Experiment

Figure 4.16 shows the prediction modelling graph using ANN for Surface Roughness versus depth of cut for single pass grinding. Table 4.1 shows the prediction for grinding using water based coolant with Silicon Carbide wheel obtained the highest correlation between target and output which is 0.996029. Meanwhile, the R-squared is 0.929258. These shows there are high relationship between the target and output graph. Table 4.2 shows the prediction for grinding using water based coolant with Al_2O_3 wheel obtained high correlation between target and output which is 0.992852. Meanwhile, the R-squared is 0.985055. These shows there are high relationship between the target and output graph.

Besides that, Table 4.3 shows the prediction for grinding using ZnO with SiC wheel obtained lowest correlation between target and output which is 0.966179. Meanwhile, the R-squared is 0.894227. These shows there are high relationship between the target and output graph. Figure 4.16 also shows the predicted surface roughness for cutting depth from 21 μm to 51 μm. The model predicted that, the surface roughness almost became constant after the cutting depth 21 μm for each of the grinding experiments in Figure 4.16. Since, there is only an insignificant increase in the surface roughness after 21 μm therefore it is assumed to be constant.
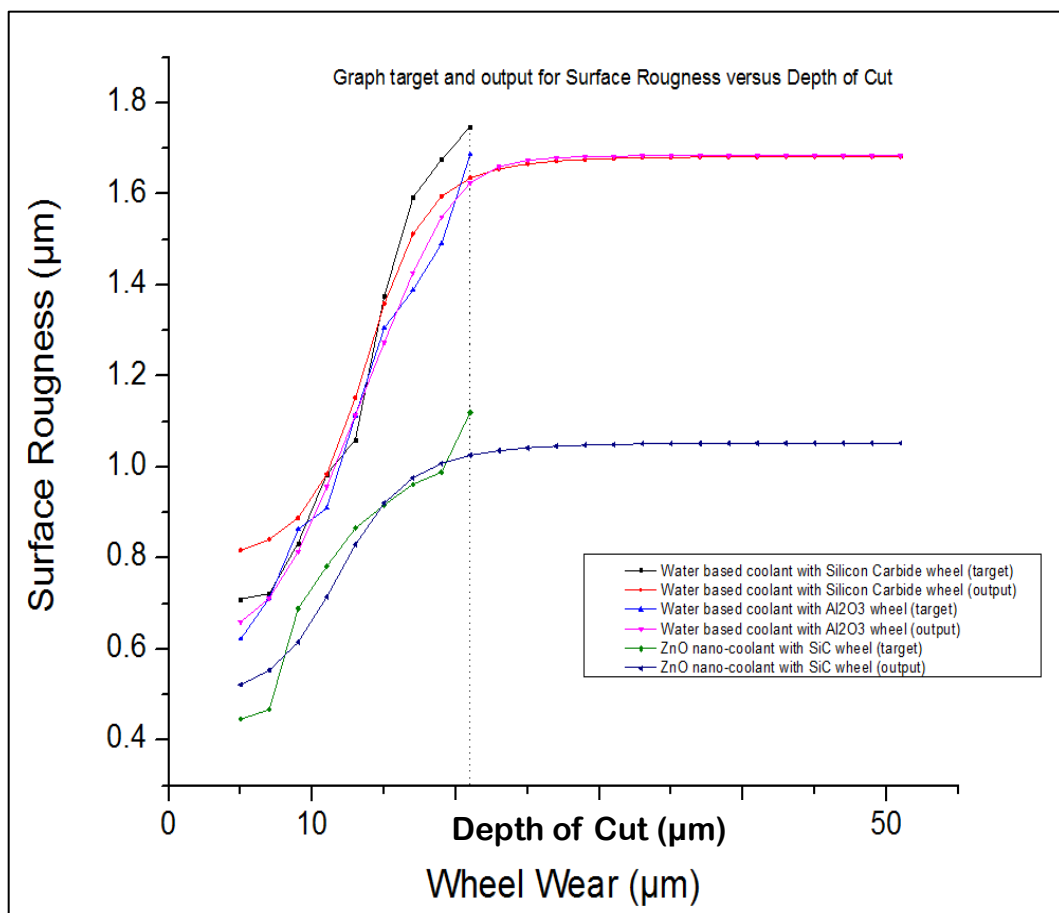
Figure 4.16: Graph of ANN Prediction for single pass grinding

Table 4.1: Summary of Prediction for Water Based Coolant with SiC Wheel Grinding for Single pass Experiment

	Target	Output	Absolute Error	Relative Error
Mean	1.189	1.198313	0.073789	0.071605
Standard Deviation	0.391572	0.31454	0.039421	0.052525
Minimum Value	0.71	0.816886	0.000037	0.000037
Maximum Value	1.748	1.635559	0.11893	0.164723
Correlation	0.996029			
R-squared	0.929258			

Table 4.2: Summary of Prediction for Water Based Coolant with Al_2O_3 Wheel Grinding for Single pass Experiment

	Target	Output	Absolute Error	Relative Error
Mean	1.121444	1.125834	0.03617	0.033075
Standard Deviation	0.348127	0.342651	0.021128	0.020827
Minimum Value	0.622	0.659391	2.09×10^{-8}	2.94×10^{-8}
Maximum Value	1.687	1.625016	0.061984	0.060114
Correlation	0.992852			
R-squared	0.985055			

Table 4.3: Summary of Prediction for ZnO Nano-Coolant with SiC Wheel Grinding for Single pass Experiment

	Target	Output	Absolute Error	Relative Error
Mean	0.804222	0.796192	0.05228	0.079059
Standard Deviation	0.218861	0.188716	0.032153	0.062284
Minimum Value	0.446	0.521369	0.003666	0.003998
Maximum Value	1.12	1.025737	0.094263	0.185242
Correlation	0.966179			
R-squared	0.894227			

4.5.2   Modeling on Multi Pass Experiment

Figure 4.17 shows the prediction modelling graph using ANN for Surface Roughness versus depth of cut for multi pass grinding. Table 4.4 shows the prediction for grinding using water based coolant with SiC wheel obtained the highest correlation between target and output which is 0.996463. Meanwhile, the R-squared is 0.98998. These shows there are high relationship between the target and output graph. Table 4.5 shows the prediction for grinding using water based coolant with Al_2O_3 wheel obtained high correlation between target and output which is 0.996356. Meanwhile, the R-squared is 0.965241. These shows there are also high relationship between the target and output graph.

Besides that, Table 4.3 shows the prediction for grinding using ZnO nano-coolant with SiC wheel obtained lowest correlation between target and output which is 0.985782. Meanwhile, the R-squared is 0.959578. These shows there also are high relationship between the target and output graph. Figure 4.17 also shows the predicted surface roughness for cutting depth from 21 μm to 51 μm. The model predicted that, the surface roughness almost became constant after the cutting depth 21 μm for each of the grinding experiments in Figure 4.16. Since, there is only an insignificant increase in the surface roughness after 21 μm therefore it is assumed to be constant.
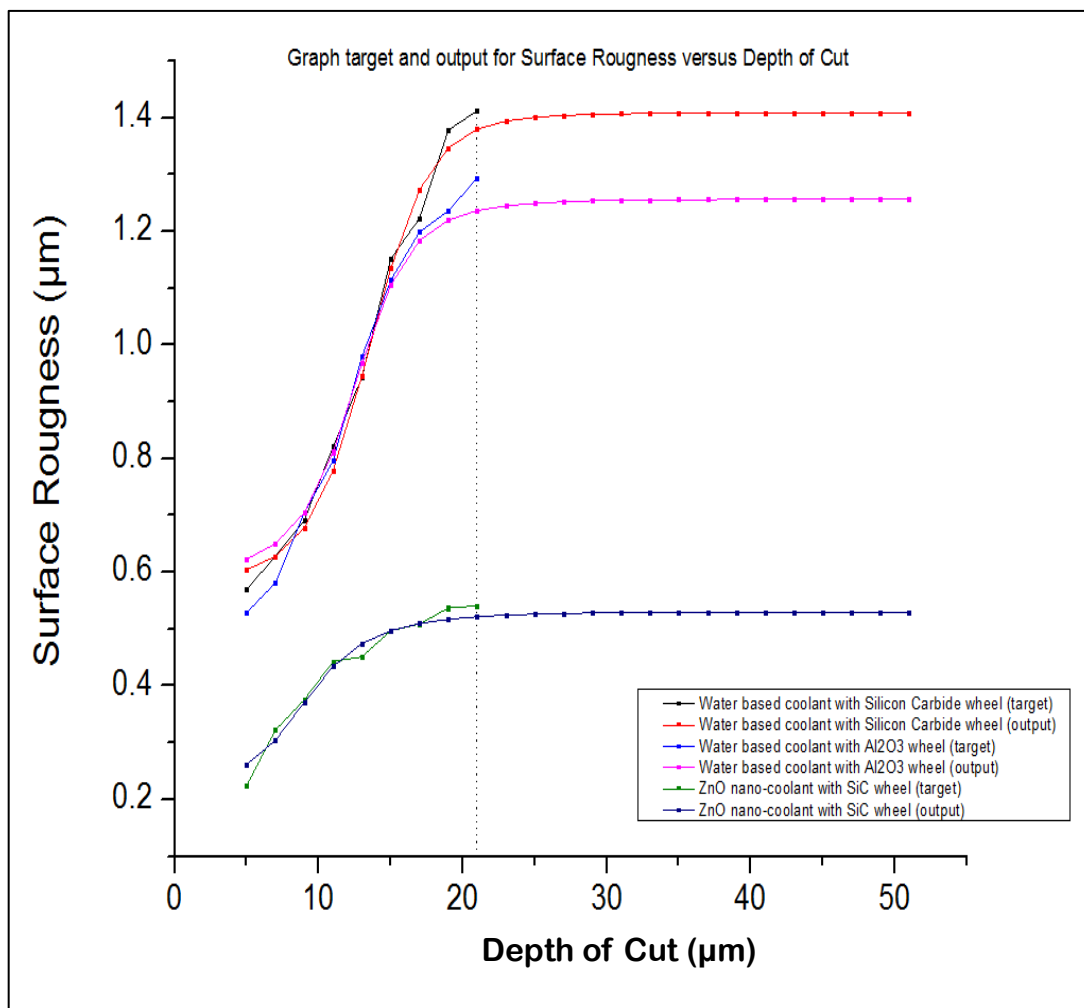
Figure 4.17: Graph of ANN Prediction for multi passes grinding

Table 4.4: Summary of Prediction for Water Based Coolant with SiC Wheel Grinding for Multi pass Experiment

	Target	Output	Absolute Error	Relative Error
Mean	0.979889	0.974337	0.024862	0.026153
Standard Deviation	0.304642	0.298557	0.016586	0.019591
Minimum Value	0.57	0.604103	3.43×10^{-8}	5.46×10^{-8}
Maximum Value	1.412	1.379629	0.050841	0.059829
Correlation	0.996463			
R-squared	0.98998			

Table 4.5: Summary of Prediction for Water Based Coolant with Al_2O_3 Wheel Grinding for Multi pass Experiment

	Target	Output	Absolute Error	Relative Error
Mean	0.936889	0.944703	0.031803	0.044941
Standard Deviation	0.275838	0.238025	0.030949	0.057974
Minimum Value	0.529	0.622848	0.00005	0.000071
Maximum Value	1.293	1.236336	0.093848	0.177406
Correlation	0.996356			
R-squared	0.965241			

Table 4.6: Summary of Prediction for ZnO Nano-Coolant with SiC Wheel Grinding for Multi pass Experiment

	Target	Output	Absolute Error	Relative Error
Mean	0.433444	0.432424	0.014565	0.041809
Standard Deviation	0.10089	0.092084	0.011428	0.047027
Minimum Value	0.225	0.261765	6.34×10^{-8}	1.28×10^{-7}
Maximum Value	0.541	0.521626	0.036765	0.1634
Correlation	0.985782			
R-squared	0.959578			

CHAPTER 5

CONCLUSION AND RECOMMENDATION

5.1   Conclusion

The overall studies of the project were about finding the effect of grinding condition which is depth of cut, type of wheel and type of grinding coolant on the surface roughness and wheel wear. Generally, the Surface Roughness for all the experiment has been increased when the cutting depth has been increased when grind P20 tool steel. Besides that, Aluminium Oxide wheel obtains better Surface Roughness compare to Silicon Carbide wheel. The mean of Surface Roughness for single pass grinding using Silicon Carbide wheel is 1.189 μm and for Aluminium Oxide wheel is 1.1214 μm. The percentage difference between these two wheels is 6.0 %. However, for multi pass experiment the percentage difference is 4.6 %.

Furthermore, Zinc Oxide Nano-coolant obtains lower Surface Roughness and wheel wear compared to Water Based coolant. The mean of Surface Roughness for single pass grinding using Zinc Oxide Nano-coolant is 0.8042 μm and for Water Based coolant is 1.189 μm. The percentage difference between Zinc Oxide Nano-coolant and Water Based coolant is 47.84 %. However, for multi pass experiment the percentage difference is much higher which 126.1 %. Moreover, the wheel wears for grinding using Water Based coolant are much higher compare to grinding using Zinc Oxide Nano-coolant. The total wheel wears for grinding using Water Based coolant is 0.69 mm but the wheel wear for grinding using Zinc Oxide Nano-coolant is insignificant.

Finally, the prediction modelling using Artificial Neural Network obtains a constant Surface Roughness for cutting depth above 21 μm. It can be concluded that the Surface Roughness are maximum at 21 μm for P20 tool Steel.

5.2   Recommendations for Future Research

Following recommendation can be implemented for future research and development on P20 tool steel machinability.

- Different concentration of Zinc Oxide Nano-coolant can be used instead of using only one concentration of coolant.
- Include work table speed as another grinding parameter instead of maintaining it as constant.
- The grinding experiment can be conducted using different sizes of nano particle to observe the variation it the results.
- CNC milling can be used as an alternative for grinding machine.

REFERENCE

Aguiar, P.R., Cruz, C.E.D., Paula, W.C.F. and Bianchi, E.C. 2008. Prediction Surface Roughness in Grinding using Neural Networks. *Advance in Robotics, Automation and Control*, **16**(9), pp. 432

Aguair, P.R., Dotto, F.R.L. and Bianchi, E.C. 2005. Study of Thresholds to Burning in Surface Grinding Process. *Journal of Braz Society of Mechanical Science and Engineering*, **27**(2), pp. 150-156.

Akiyama, T., Shibata, S. and Yonetsu, D. 1984. Behaviour of grinding fluid in the gap of the contact area between wheel and workpiece. *Proceeding of the 5ᵗʰ International Conference Product Engineering*.

Bhatesa, C.P., Chisholm, A.W.J., and Pattinson, E.J. 1972. Advance Grinding Technology. *Proceeding of the International Grinding Conference*, pp. 334-339.

Brinksmeier, E., Heinzel, C. and Wittmann, M. 1999. Friction and Lubrication in Grinding. *Journal of Manufacturing Technology*, **48**(2), pp. 581-598.

Buttery, T.C., Statham, A., Percival, J.B. and Hamed, M.S. 1979. Some Effect of Dressing on Grinding Performance. *Journal of Mechanical and Production Engineering*, **55**(1979), pp. 195-219.

Campbell, J.D. 1995. Optimized coolant application. *1ˢᵗ International Machining and Grinding Conference*, pp. 12-14.

Chen, X., Allanson, D.R. and Rowe, W.B. 1998. Life cycle model of the grinding process. *Journal of Computer Industry*, **36**(5), pp. 5-11.

Chen, X. and Rowe, W.B. 1995. Analysis and Simulation of the Grinding Process. *International Journal of Machining Tool Manufacturing*, **36**(8), pp. 883-896.

Choi, S.U. 1995. Enhancing thermal conductivity of fluids with nanoparticles. *Proceeding of the ASME International Mechanical Engineering Congress.*

Ebbrell, S., Wooley, N.H., Tridimas, T.D., Allanson, D.R. and Rowe, W.B. 1999. The effects of cutting fluid application method on the grinding process. *International Journal of Machine Tool and Manufacture*. **40**(2000), pp. 209-223.

Farhat, Z.N. 2003. Wear mechanism of CBN cutting tool during high-speed machining of mold steel. *Journal of Material Science and Engineering*, **61**(5), pp. 101-109.

Hecker, R.L. and Liang, S.Y. 2003. Predictive modelling of surface roughness in grinding. *International Journal of Machine Tools and Manufacturing*, **43**(2003), pp. 755-761.

Hryniewicz, P., Szeril, A.Z. and Jahanmir, S. 1998. Coolant flow in surface grinding with non-porous wheels. *International Journal of Mechanical Science*, **42**(2000), pp. 2347-2367.

Incropera, F.P. and DeWitt, D.P. 2001. Fundamental of heat and Mass Transfer. New York: Wiley.

Kamely, M.A., Kamil, S.M. and Chong, C.W. 2011. Mathematical Modeling of Surface Roughness in Surface Grinding Operation. *World Academy of Science and Engineering*, pp. 1048-1051.

Krajnik, P., Kopac, J. and Sluga, A. 2005. Design of grinding factor based on response surface methodology. *Journal of Material Technology*, **163**(2005), pp. 629-636.

Krishna, J., Reddy, S. and Reddy, V.K. 2004. Modelling of Machining Parameters in CNC End Milling using Pricipal Component Analysis Based Neural Networks. *Innovative System Design and Engineering*, **2**(3), pp. 223-234.

Ling, Y., 2001. Low-Damage Grinding or Polishing of Silicon Carbide Surface. *Journal of Precision Machining*, **3**(1), pp. 1-8.

Madl, J. 2009. Design of Machining. *Journal of Manufacturing Technology*, **9**(4), pp. 81-86.

Madl, J., Jersak, J. and Holesovsky, F. 2003. Quality of Machining. *Journal of Manufacturing Technology*, pp. 12-14.

Malkin, S. 1989. Theory and Application of Machining with Abrasives. *Journal Grinding Technology*, pp.43-49.

Malkin, S. 1989. *Theory and application of machining with abrasives*. New York: John Wiley and Sons.

Midha, P.S., Zhu, C.B. and Trmal, G.J. 1991. Optimum Selection of Grinding Parameter Using Process Modelling and Knowledge Based System Approach. *Journal of Processing Technology,* **28**(3), pp. 189-198.

Oliveira, J.F.G., Silva, E.J., Guo, C. and Hashimoto, F. 2009. Industrial challenges in grinding. *Journal of Manufacturing Technology*, **58**(2), pp. 663-680.

Outwater, J.O. and Shaw, M.C. 1952. Surface temperature in grinding. *Trans of ASME*, **74**(4), pp. 73-86.

Pahlitzsch, G. and Appun, J. 1954. Internal Diamond Revolution. *Journal of Creative Manufacturing*, pp. 566-569.

Pande, S.J., Halder, S.N. and Lal, G.K. 1979. Evaluation of grinding wheel performance. *Department of Mechanical Engineering*, **58**(1980), pp. 337-248.

Pande, S.J. and Lal, G.K. 1975. Wheel Wear in Dry Surface Grinding. *International Journal of Machine Tool Dressing Research*, **16**(4), pp. 179-186.

Pang, J.Z., Wang, M.J. and Duan, C.Z. 2001. White layer and surface roughness in high speed milling of P20 steel. *Journal of Precision and Non-Traditional Machining Technology*, pp. 212-234.

Safian, S., Hisham, M.A. and Aman, S. 2009. Evaluation of vegetable oil as an Alternative cutting lubricant when end milling martensutic stainless steel using uncoated carbide tool. *Journal of Advance Manufacturing and Technology*, **3**(2), pp. 49-55.

Saidur, R., Leong, K.Y. and Mahammad, H.A. 2011. Areview on applications and challenges of nanofluids. *Journal of Renewable and Sustainable Energy*, **15**(4), pp. 1646-1668.

Samek, D., Bilek, O. and Cerny, J. 2011. Prediction of grinding parameter for plastic by artificial neural networks. *International Journal of Mechanics*, **3**(5), pp. 250-261.

Sedlacek, M., Podgornik, B. and Vizintin, J. 2008. Infuence of surface preparation on roughness parameter. *Journal of Wear*, **266**(45), pp. 482-487.

Shaji, S. and Radhakrishnan, V. 2002. Analysis of process parameter in surface grinding with graphite as lubricant based on the Taguchi Method. *Journal of Materials Processing Technology*, **141**(2003), pp. 51-59.

Shen, B., Shih, A.J. and Tung, S.C. 2008. Appication of Nanofluid in Minimum Quantity Lubricant Grinding. *Society of tribologist and lubricant engineers*, **51**(5), pp. 737-737.

Trmal, G. and Kaliszer, H. 1976. Delivery of cutting fluid in grinding. *Journal of Advance Machining*, pp. 52-57.

Uslu, I., Comert, H., Ipek, M., Celebi. F.G., Ozdemir, O. and Bindal, C. 2006. A comparison of borides formed on AISI 1040 and AISI P20 steel. *Journal of Material and Design*, **28**(2), pp. 1819-1826.

Webster, J.A., Cui, C. and Mindek, R.B. 1995. Grinding Fluid Application System Design. *Centre for Research and Development University of Connecticut*, **44**(1), pp. 333-338.

Webster, J.A., Hilez, C. and Mindek, J. 1989. Grinding fluid application system design. *Annals of the CIRP*. **4**(1), pp. 333-338.

Wieczorowski, K., Legutko, S. and Kedzierski, T. 2006. Investigation of the Influence of Grinding Parameters on the Errors and Surface Roughness of Holes. *Scientific Bulletin of the Petru Maior University of Targu Mures*, **2**(19), pp, 31-38.

Xie, G.Z. and Huang, H. 2008. An experimental investigation of temperature in high speed deep grinding of partially stabilized zirconia. *Journal of Machine Tool and Manufacture*, **48**(4), pp. 1562-1568.

Yanyan, Y., Bo, Z. and Junli, L. 2009. Ultraprecision surface finishing of nano-ZrO_2 ceramics using two-dimensional ultrasonic assisted grinding. *International Journal of Advance Manufacturing Technology*, **43**(10), pp. 462-467.

Zhong, Z.W. 2003. Grinding of Aluminum-Based Metal Matrix Composites Reinforced with Al_2O_3 or SiC Particles. *International Journal of Advance Manufacturing Technology*, **21**(79), pp. 80-85.

Zhou, X., and Xi, F. 2002. Modeling and prediction surface roughness of grinding process. International *Journal of Machine and Manufacture*, **42**(8), pp. 969-977.

APPENDIX A1

Gantt chart for Final Year Project 1

Project Activities	Semester 1														
	Week 1	Week 2	Week 3	Week 4	Week 5	Week 6	Week 7	Midterm Break	Week 8	Week 9	Week 10	Week 11	Week 12	Week 13	Week 14	Week 15
Research on topic	▓	▓	▓	▓												
Literature Review				▓	▓	▓	▓	▓	▓	▓	▓	▓				
Designing Of Experiment								▓	▓	▓	▓	▓				
Training (machine Handling)												▓	▓			
Run experiment													▓	▓	▓	▓
Presentation															▓	▓

APPENDIX A2

Gantt chart for Final Year Project 2

Project Activities	Semester 2															
	Week 1	Week 2	Week 3	Week 4	Week 5	Week 6	Week 7	Midterm Break	Week 8	Week 9	Week 10	Week 11	Week 12	Week 13	Week 14	Week 15
Run experiment	X	X	X	X	X	X	X									
Validation of data								X	X	X						
Data analysis										X	X	X	X			
Documentation													X	X		
Thesis writing		X	X	X	X	X	X	X				X	X	X	X	
Presentation															X	X

APPENDIX B1

Water Based Coolant Grinding Experimental Results

Grinding Condition	
Grinding Wheel	SiC
Grinding passes	1 pass

Depth of Cut, µm	Wheel Diameter, mm			Surface Roughness(Ra),µm			
	Initial	Final	Wheel wear	1	2	3	mean
5	157.70	15.70	-	0.876	0.711	0.543	**0.710**
7	155.50	155.50	-	0.882	0.638	0.646	**0.722**
9	155.38	155.38	-	1.114	0.554	0.831	**0.833**
11	155.18	155.16	**0.02**	1.179	0.681	1.092	**0.984**
13	154.97	154.95	**0.02**	1.243	0.745	1.192	**1.060**
15	154.88	154.84	**0.04**	1.134	1.323	1.671	**1.376**
17	154.82	154.76	**0.06**	1.614	1.437	1.725	**1.592**
19	154.71	154.65	**0.06**	1.602	1.722	1.704	**1.676**
21	154.61	154.53	**0.08**	1.825	1.726	1.693	**1.748**

Grinding Condition	
Grinding Wheel	SiC
Grinding passes	4 pass

Depth of Cut, μm	Wheel Diameter, mm			Surface Roughness(Ra),μm			
	Initial	Final	Wheel wear	1	2	3	mean
5	203.48	203.48	-	0.330	0.916	0.464	**0.570**
7	203.48	203.48	-	0.428	0.704	0.752	**0.628**
9	203.48	203.46	**0.02**	0.542	0.706	0.828	**0.692**
11	203.46	203.44	**0.02**	0.751	0.731	0.981	**0.821**
13	203.44	203.40	**0.04**	0.930	0.926	0.973	**0.943**
15	202.54	202.48	**0.06**	1.073	0.889	1.494	**1.152**
17	202.48	202.40	**0.08**	1.013	1.135	1.521	**1.223**
19	202.40	202.31	**0.09**	1.123	1.458	1.553	**1.378**
21	202.31	202.21	**0.10**	1.146	1.584	1.506	**1.412**

Grinding Condition	
Grinding Wheel	Al_2O_3
Grinding passes	1 pass

Depth of Cut, µm	Wheel Diameter, mm			Surface Roughness(Ra),µm			
	Initial	Final	Wheel wear	1	2	3	mean
5	188.68	188.64	**0.04**	0.681	0.543	0.642	**0.622**
7	188.64	188.58	**0.06**	0.813	0.548	0.775	**0.712**
9	188.58	188.46	**0.10**	0.952	0.820	0.817	**0.863**
11	187.54	188.40	**0.14**	0.704	0.933	1.093	**0.910**
13	187.38	187.22	**0.16**	0.851	1.344	1.144	**1.113**
15	187.21	187.01	**0.20**	1.246	1.236	1.436	**1.306**
17	186.44	186.24	**0.20**	1.233	1.454	1.480	**1.389**
19	186.24	186.02	**0.22**	1.459	1.476	1.538	**1.491**
21	185.22	184.94	**0.28**	1.771	1.531	1.759	**1.687**

	Grinding Condition	
Grinding Wheel	Al_2O_3	
Grinding passes	4 pass	

Depth of Cut, µm	Wheel Diameter, mm			Surface Roughness(Ra),µm			
	Initial	Final	Wheel wear	1	2	3	mean
5	193.28	193.22	**0.06**	0.532	0.467	0.588	**0.529**
7	193.22	193.12	**0.10**	0.633	0.498	0.612	**0.581**
9	193.12	193.00	**0.12**	0.556	0.672	0.887	**0.705**
11	191.88	191.76	**0.12**	0.722	0.887	0.779	**0.796**
13	191.76	191.58	**0.18**	0.799	1.121	1.017	**0.979**
15	191.58	191.36	**0.22**	1.022	1.098	1.222	**1.114**
17	190.74	190.48	**0.26**	1.022	1.308	1.267	**1.199**
19	190.48	190.20	**0.28**	1.342	1.126	1.240	**1.236**
21	190.20	189.82	**0.38**	1.173	1.255	1.451	**1.293**

APPENDIX B2

ZnO Nano-Coolant Grinding Experimental Results

Grinding Condition	
Grinding Wheel	SiC
Grinding passes	1 pass

Depth of Cut, μm	Wheel Diameter, mm			Surface Roughness(Ra),μm			
	Initial	Final	Wheel wear	1	2	3	mean
5	166.45	166.45	-	0.421	0.501	0.416	**0.446**
7	166.40	166.40	-	0.459	0.523	0.419	**0.467**
9	166.36	166.36	-	0.857	0.627	0.583	**0.689**
11	166.24	166.24	-	0.894	0.759	0.693	**0.782**
13	165.83	165.83	-	0.739	0.942	0.917	**0.866**
15	165.72	165.72	-	1.012	0.891	1.010	**0.917**
17	165.62	165.62	-	0.968	0.891	1.027	**0.962**
19	165.51	165.51	-	1.102	0.945	0.920	**0.989**
21	165.02	165.02	-	1.025	1.092	1.243	**1.120**

Grinding Condition	
Grinding Wheel	SiC
Grinding passes	4 pass

Depth of Cut, µm	Wheel Diameter, mm			Surface Roughness(Ra),µm			
	Initial	Final	Wheel wear	1	2	3	mean
5	163.23	163.23	-	0.193	0.332	0.150	**0.225**
7	163.16	163.16	-	0.284	0.423	0.259	**0.322**
9	163.11	163.11	-	0.320	0.401	0.407	**0.376**
11	162.79	162.79	-	0.338	0.427	0.564	**0.443**
13	162.60	162.60	-	0.442	0.399	0.512	**0.451**
15	162.53	162.53	-	0.448	0.562	0.481	**0.497**
17	162.00	162.00	-	0.553	0.632	0.342	**0.509**
19	161.90	161.90	-	0.488	0.521	0.602	**0.537**
21	161.79	161.79	-	0.548	0.532	0.543	**0.541**

APPENDIX C1

SEM photograph for water based coolant grinding with cutting depth 5 µm and SiC wheel
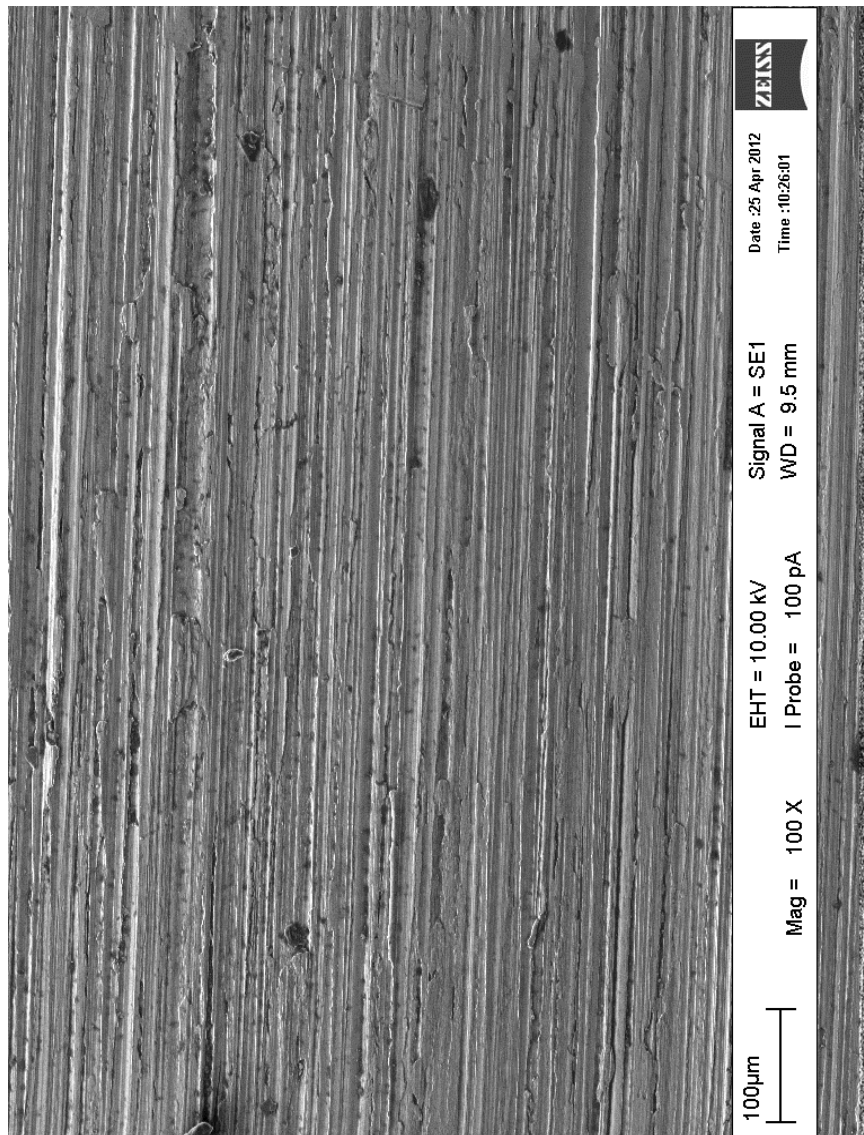
APPENDIX C2

SEM photograph for water based coolant grinding with cutting depth 11 μm and SiC wheel
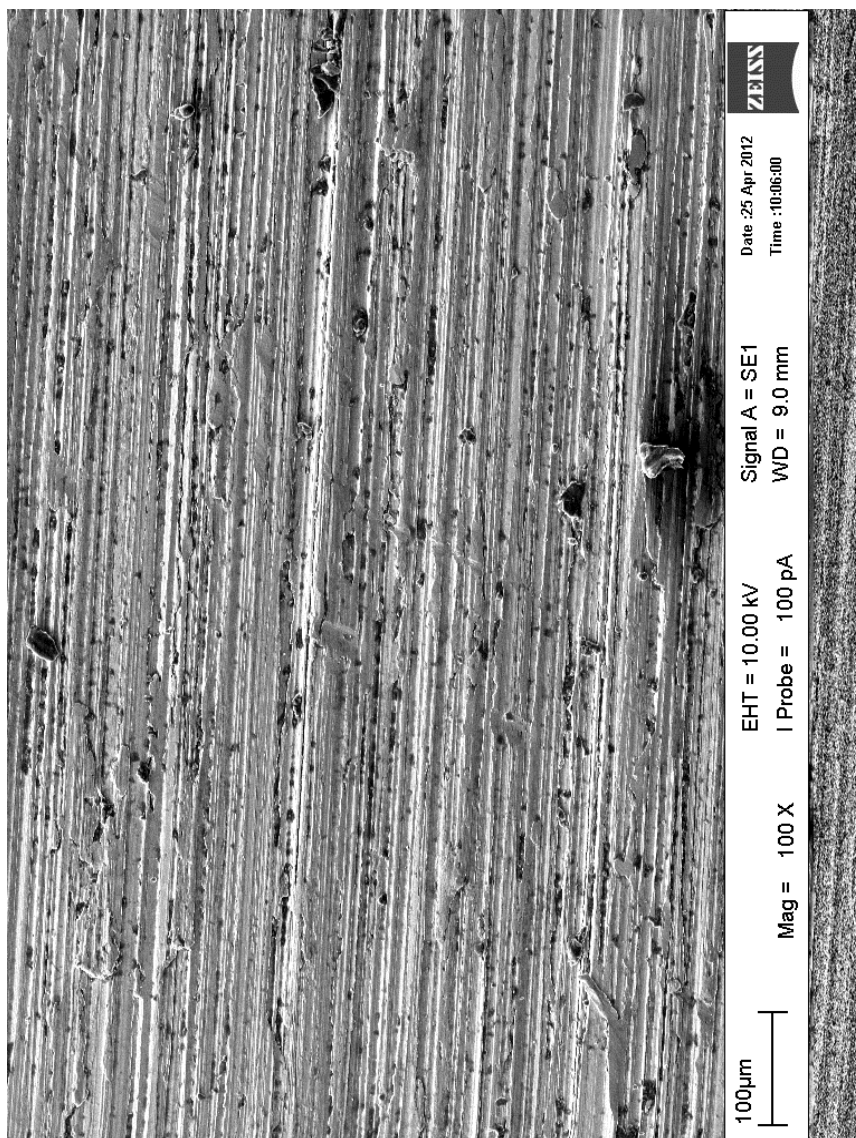
APPENDIX C3

SEM photograph for water based coolant grinding with cutting depth 21 μm and SiC wheel
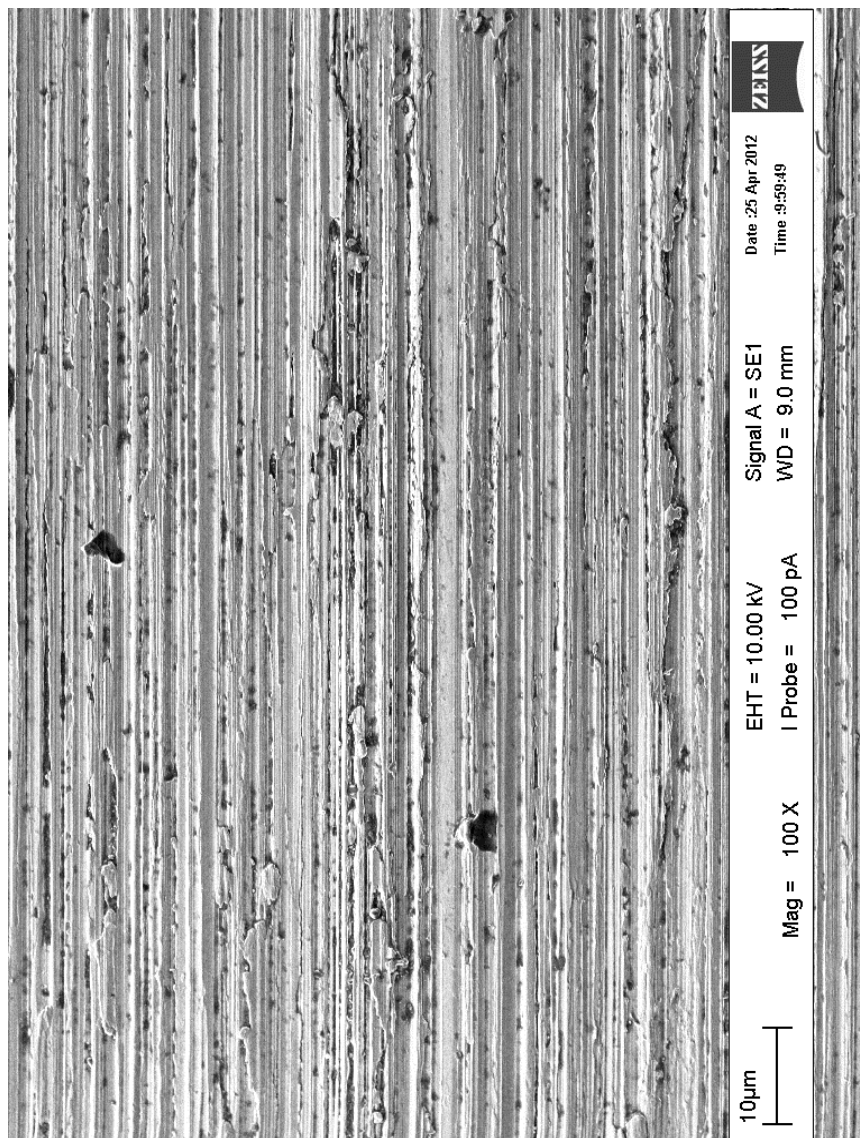
APPENDIX D1

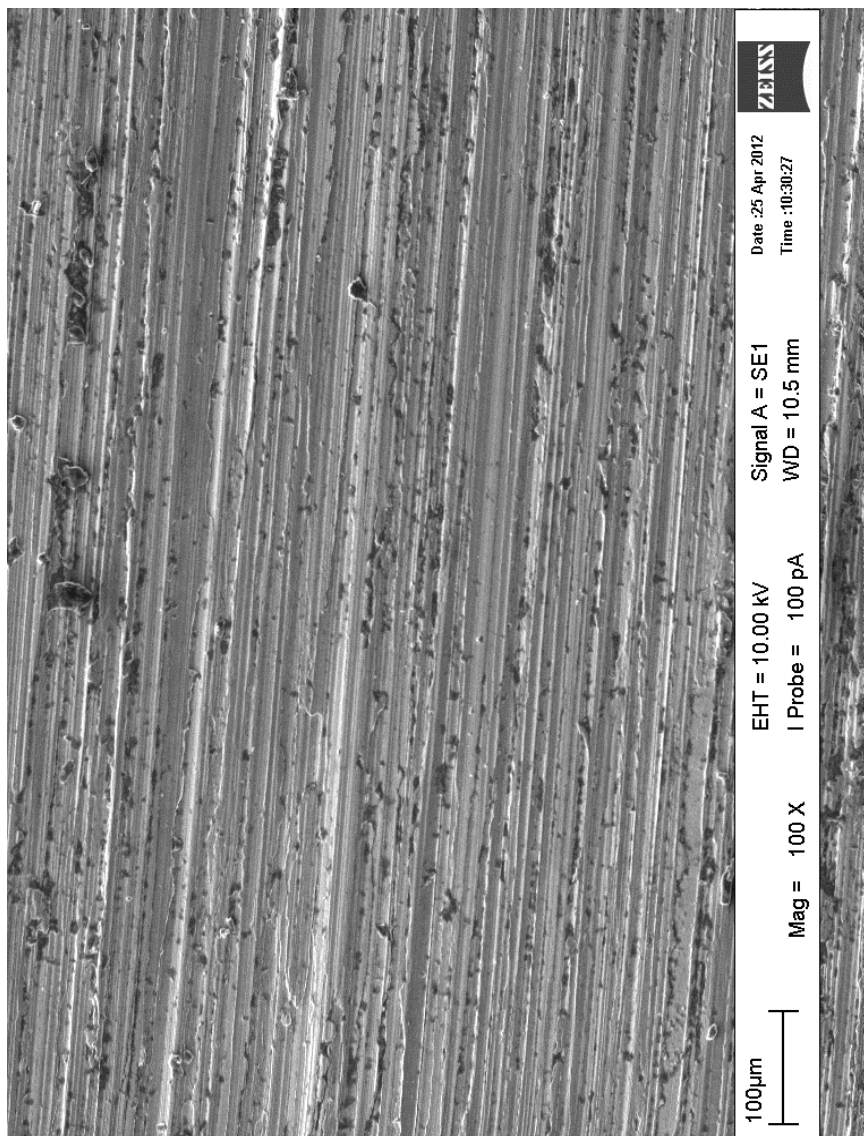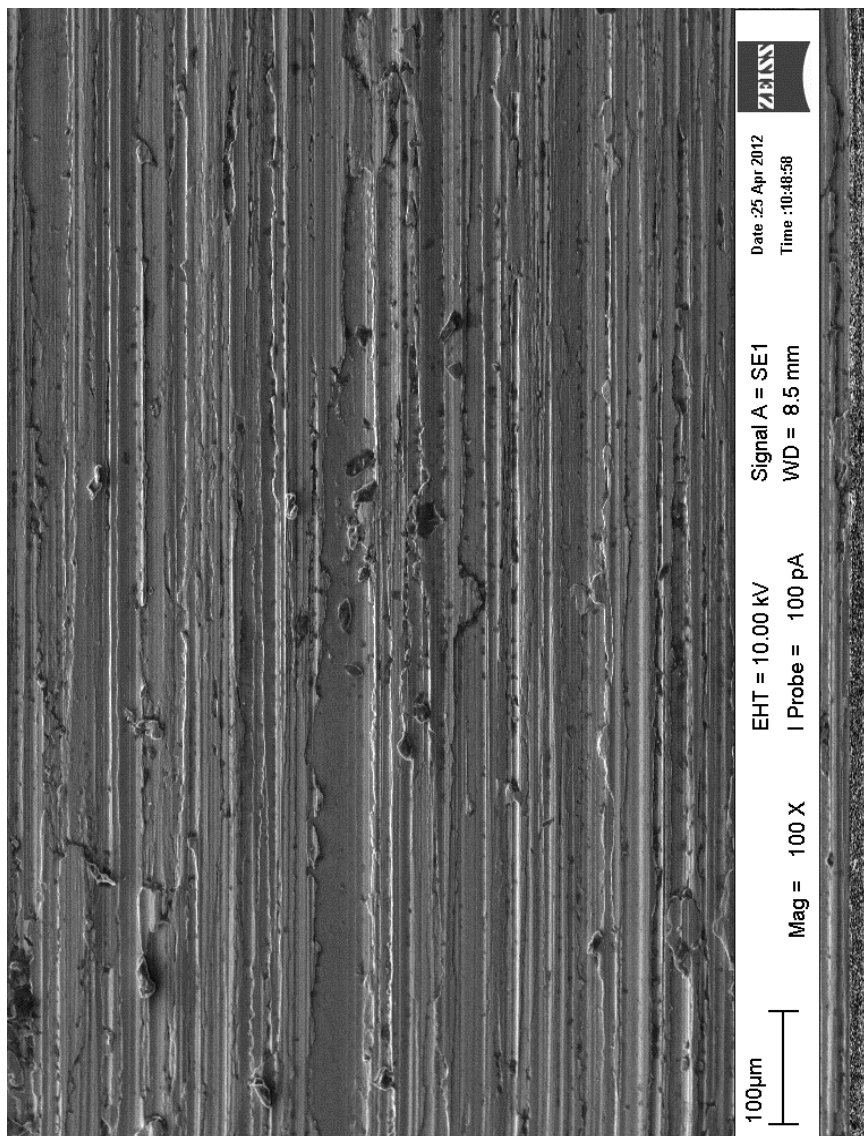**SEM photograph for ZnO Nano-coolant grinding with cutting depth 5 µm and SiC wheel**
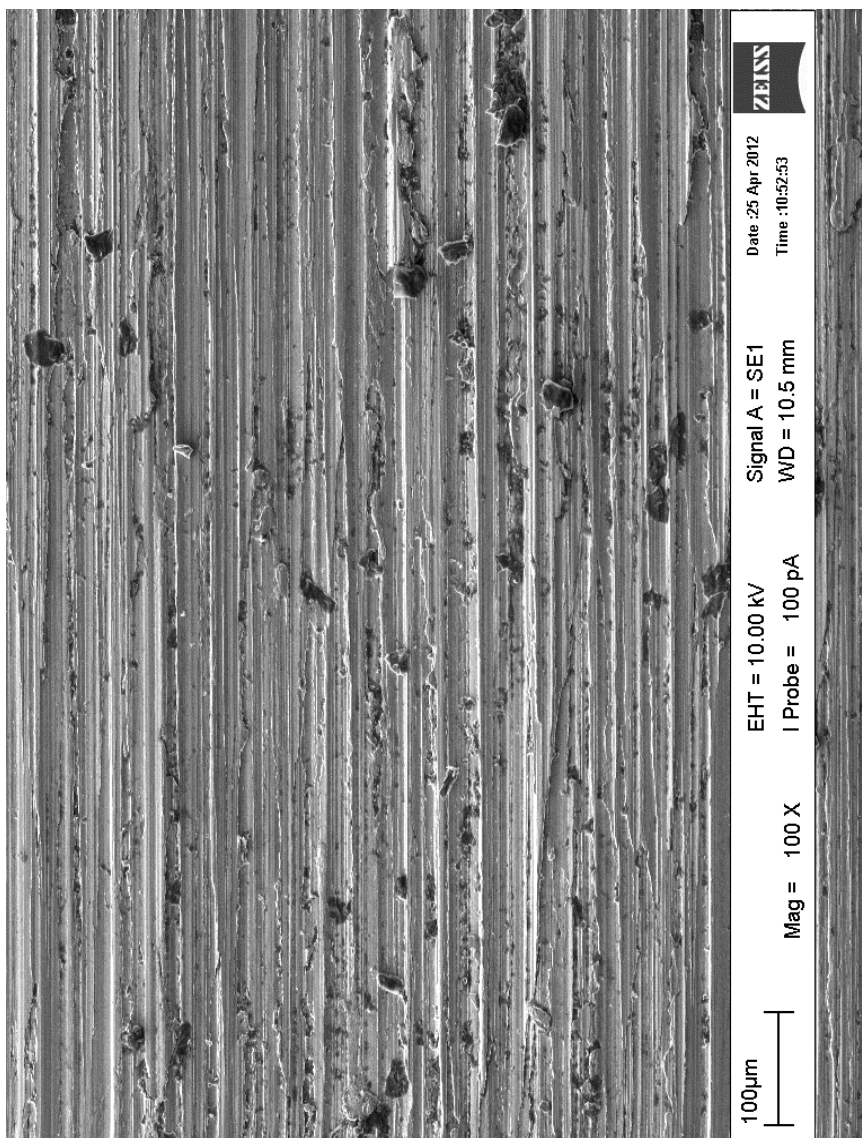
APPENDIX D2

SEM photograph for ZnO Nano-coolant grinding with cutting depth 11 μm and SiC wheel

APPENDIX D3

SEM photograph for ZnO Nano-coolant grinding with cutting depth 21 μm and SiC wheel

APPENDIX E1

ANN Modeling Results for water based coolant grinding with Al$_2$O$_3$ wheel

Single pass					Multi pass				
Depth of Cut	Target	Output	AE	ARE	Depth of Cut	Target	Output	AE	ARE
5	0.622	0.659391	0.037391	6.011438	5	0.529	0.622848	0.093848	17.74057
7	0.712	0.712	2.09E-08	0.000003	7	0.581	0.650067	0.069067	11.88757
9	0.863	0.813971	0.049029	5.681193	9	0.705	0.70505	0.00005	0.007054
11	0.91	0.956712	0.046712	5.133233	11	0.796	0.811315	0.015315	1.924029
13	1.113	1.114286	0.001286	0.1155	13	0.979	0.967411	0.011589	1.183767
15	1.306	1.274002	0.031998	2.450061	15	1.114	1.105976	0.008024	0.720288
17	1.389	1.426995	0.037995	2.735422	17	1.199	1.183706	0.015294	1.275538
19	1.491	1.550134	0.059134	3.966081	19	1.236	1.219619	0.016381	1.325292
21	1.687	1.625016	0.061984	3.674238	21	1.293	1.236336	0.056664	4.382364
23	-	1.660032	-	-	23	-	1.244724	-	-
25	-	1.674216	-	-	25	-	1.249273	-	-
27	-	1.679886	-	-	27	-	1.2519	-	-
29	-	1.682306	-	-	29	-	1.253491	-	-
31	-	1.683432	-	-	31	-	1.254486	-	-
33	-	1.683997	-	-	33	-	1.255124	-	-
35	-	1.684298	-	-	35	-	1.25554	-	-
37	-	1.684463	-	-	37	-	1.255814	-	-
39	-	1.684556	-	-	39	-	1.255996	-	-
41	-	1.684609	-	-	41	-	1.256117	-	-
43	-	1.68464	-	-	43	-	1.256199	-	-
45	-	1.684658	-	-	45	-	1.256254	-	-
47	-	1.684668	-	-	47	-	1.256291	-	-
49	-	1.684674	-	-	49	-	1.256316	-	-
51	-	1.684677	-	-	51	-	1.256333	-	-

APPENDIX E2

ANN Modeling Results for water based coolant grinding with SiC wheel

Single pass					Multi pass				
Depth of Cut	Target	Output	AE	ARE	Depth of Cut	Target	Output	AE	ARE
5	0.71	0.816886	0.106886	15.054422	5	0.57	0.604103	0.034103	5.982913
7	0.722	0.84093	0.11893	16.472277	7	0.628	0.628	3.43E-08	0.000005
9	0.833	0.888481	0.055481	6.660355	9	0.692	0.678219	0.013781	1.991541
11	0.984	0.984037	0.000037	0.003718	11	0.821	0.778842	0.042158	5.13497
13	1.06	1.152628	0.092628	8.738504	13	0.943	0.944948	0.001948	0.206608
15	1.376	1.358345	0.017655	1.283082	15	1.152	1.134553	0.017447	1.514526
17	1.592	1.512603	0.079397	4.987219	17	1.223	1.273841	0.050841	4.157067
19	1.676	1.595349	0.080651	4.812108	19	1.378	1.346895	0.031105	2.257224
21	1.748	1.635559	0.112441	6.43253	21	1.412	1.379629	0.032371	2.29255
23	-	1.65571	-	-	23	-	1.393995	-	-
25	-	1.666476	-	-	25	-	1.400614	-	-
27	-	1.672578	-	-	27	-	1.403894	-	-
29	-	1.676199	-	-	29	-	1.405638	-	-
31	-	1.67842	-	-	31	-	1.406622	-	-
33	-	1.679815	-	-	33	-	1.407204	-	-
35	-	1.680706	-	-	35	-	1.407559	-	-
37	-	1.681281	-	-	37	-	1.40778	-	-
39	-	1.681657	-	-	39	-	1.407921	-	-
41	-	1.681903	-	-	41	-	1.408011	-	-
43	-	1.682065	-	-	43	-	1.408069	-	-
45	-	1.682173	-	-	45	-	1.408107	-	-
47	-	1.682244	-	-	47	-	1.408132	-	-
49	-	1.682291	-	-					
51	-	1.682322	-	-					

APPENDIX F

ANN Modeling Results for ZnO nano-coolant grinding with SiC wheel

Single pass					Multi pass				
Depth of Cut	Target	Output	AE	ARE	Depth of Cut	Target	Output	AE	ARE
5	0.446	0.487381	0.041381	9.278187	5	0.225	0.261765	0.036765	16.33998
9	0.689	0.67035	0.01865	2.706819	7	0.322	0.304221	0.017779	5.521321
11	0.782	0.781999	7.76E-07	0.000099	9	0.376	0.371526	0.004474	1.18991
13	0.866	0.862075	0.003925	0.45319	11	0.443	0.43436	0.00864	1.950328
15	0.917	0.926452	0.009452	1.030702	13	0.451	0.474489	0.023489	5.208266
17	0.962	0.987208	0.025208	2.620337	15	0.497	0.497	6.34E-08	0.000013
19	0.989	1.03931	0.05031	5.086949	17	0.509	0.509698	0.000698	0.137217
21	1.12	1.073652	0.046348	4.138211	19	0.537	0.51713	0.01987	3.700097
23	-	1.091592	-	-	21	0.541	0.521626	0.019374	3.581205
25	-	1.100015	-	-	23	-	0.524414	-	-
27	-	1.103929	-	-	25	-	0.526176	-	-
29	-	1.105793	-	-	27	-	0.527307	-	-
31	-	1.106701	-	-	29	-	0.52804	-	-
33	-	1.107152	-	-	31	-	0.52852	-	-
35	-	1.107378	-	-	33	-	0.528836	-	-
37	-	1.107491	-	-	35	-	0.529044	-	-
39	-	1.107549	-	-	37	-	0.529182	-	-
41	-	1.107578	-	-	39	-	0.529274	-	-
43	-	1.107592	-	-	41	-	0.529335	-	-
45	-	1.1076	-	-	43	-	0.529376	-	-
47	-	1.107603	-	-	45	-	0.529403	-	-
49	-	1.107605	-	-	47	-	0.529421	-	-
51	-	1.107606	-	-	49	-	0.529433	-	-
					51	-	0.529441	-	-